

Solar neutrinos and 1-3 leptonic mixing

Subabati Goswami¹, Alexei Yu. Smirnov^{2;3},

¹Harish-Chandra Research Institute, Chhatnag Road, Jhusi, Allahabad 211 019, India,

²The Abdus Salam International Centre for Theoretical Physics, I-34100, Trieste, Italy

³Institute for Nuclear Research, Russian Academy of Sciences, Moscow, Russia

Abstract

Effects of the 1-3 leptonic mixing on the solar neutrino observables are studied and the signatures of non-zero θ_{13} are identified. For this we have re-derived the formula for 3 - survival probability including all relevant corrections and constructed contours of constant values of observables in the $\sin^2 \theta_{12}$ - $\sin^2 \theta_{13}$ plane. A analysis of the solar neutrino data gives $\sin^2 \theta_{13} = 0.02^{+0.05}_{-0.02}$ (1 σ) for $m^2 = 8 \cdot 10^5 \text{ eV}^2$. The combination of the ratio CC/NC at SNO and gallium production rate selects $\sin^2 \theta_{13} = 0.034 \pm 0.026$ (1 σ). The global fit of all oscillation data leads to the best value $\sin^2 \theta_{13} = 0.004$. The sensitivity of future solar neutrino studies to $\sin^2 \theta_{13}$ can be improved down to 0.01 - 0.02 (1 σ) by precise measurements of the pp-neutrino flux and the CC/NC ratio as well as spectrum distortion at high ($E > 5 \text{ MeV}$) energies. We show that combination of experimental results sensitive to the low and high energy parts of the solar neutrino spectrum resolves the degeneracy of angles θ_{13} and θ_{12} . Comparison of $\sin^2 \theta_{13}$ as well as $\sin^2 \theta_{12}$ measured in the solar neutrinos and in the reactor/accelerator experiments may reveal new effects which can not be seen otherwise.

1 Introduction

Determination of the 1-3 mixing parameterized by the angle θ_{13} is of great importance for phenomenology, for future experimental programs, and eventually, for understanding the underlying physics.

At present, for $\sin^2 \theta_{13}$ we only have the upper bounds. The CHOOZ [1] reactor experiment (see also Palo Verde [2]) gives

$$\sin^2 \theta_{13} < 0.03; \quad 90\% \text{ C.L.} \quad (1)$$

The recent global fit of the oscillation results which includes also the solar, KamLAND and atmospheric neutrino data leads to [3, 4, 5]

$$\sin^2 \theta_{13} = 0.02 (0.05); \quad 90\% (3 \sigma) \text{ C.L.} \quad (2)$$

In [6] even stronger upper bound is quoted: $\sin^2_{13} = 0.041$ (3 σ). The bound follows mainly from the CHOOZ and atmospheric neutrino data. Their combined fit gives [5]:

$$\sin^2_{13} = 0.029 (0.067); \quad 90\% \text{ (3 } \sigma) \text{ C.L.} \quad (3)$$

(See also [7].)

Future long baseline experiments are geared towards precision measurement of θ_{13} . MINOS [8] and CERN to Gran-Sasso [9] alone will be able to only slightly improve the limit (2) down to

$$\sin^2_{13} = 0.015; \quad 90\% \text{ C.L.} \quad (4)$$

J-PARC [10] accelerator experiment will have substantially higher sensitivity:

$$\sin^2_{13} = 0.0015; \quad 90\% \text{ C.L.}; \quad (5)$$

but when all correlations and degeneracies of parameters are taken into account the estimated sensitivity reduces to $\sin^2_{13} = 0.006$ (90% C.L.) [11].

The Double-CHOOZ reactor experiment [12] will be able to improve the bound down to

$$\sin^2_{13} = 0.008; \quad 90\% \text{ C.L.} \quad (6)$$

for $m^2 = 2.4 \cdot 10^3 \text{ eV}^2$. It provides a clean channel of measurement of θ_{13} complementary to accelerator measurements [13],[11].

Detection of neutrinos from the Galactic supernova can, in principle, probe \sin^2_{13} down to $10^{-5} - 10^{-6}$. The problem here is large uncertainties in the original neutrino fluxes. Essentially one can find whether \sin^2_{13} is larger or smaller than 10^{-3} . Both the upper and the lower bounds on \sin^2_{13} may be established if \sin^2_{13} is in the range $10^{-5} - 10^{-3}$ [14].

Ultimate sensitivity, $\sin^2_{13} = 10^{-4} - 10^{-5}$, can be achieved at the neutrino factories [15].

Inference of the 1-3 mixing on the solar neutrino fluxes has been considered in a number of publications before [16] - [?]. The present solar neutrino data are not precise enough to probe \sin^2_{13} in the allowed range (2,3). Indeed, the recent analysis of the solar data alone gives

$$\sin^2_{13} = 0.075 (0.23); \quad 90\% \text{ (3 } \sigma) \text{ C.L.} \quad (7)$$

which is much weaker than the bound (3). In [5] it is found that inclusion of the latest KamLAND data improves the bound substantially due to better measurements of the total rate of events: $\sin^2_{13} = 0.041 (0.079); \quad 90\% \text{ (3 } \sigma)$.

The 1-3 mixing taken at the present upper bound modifies the allowed region of the parameters $\sin^2_{12} - m^2_{21}$ obtained from the global fit. It shifts the region toward larger m^2_{21} and smaller \sin^2_{12} , however the shift of the best fit point is within 1% [5].

It was noticed that the Earth matter regeneration effect has strong dependence on θ_{13} , as $P \propto \cos^6 \theta_{13}$ [32]. This can be used to determine θ_{13} in future solar neutrino experiments [32, 33]. Measurements of the pp-neutrino fluxes will also improve the sensitivity to \sin^2_{13} [18].

In this paper we study in details possible effects of 1-3 mixing on the solar neutrino observables. We analyze the present determination of θ_{13} and θ_{12} and evaluate the sensitivity of future solar neutrino experiments to θ_{13} .

The paper is organized as follows. We first (sec. 2) re-derive the ν_e survival probability including all relevant corrections and estimating accuracy of the approximations. We consider dependence of the probability on $\sin^2 \theta_{13}$. In sec. 3 we find simple analytic expressions for the probability in the high and low energy limits. In sec. 4 we introduce the $\sin^2 \theta_{12}$ vs $\sin^2 \theta_{13}$ plots and derive the equations for contours of constant values of observables in this plot. In sec. 5 we find the allowed region of parameters $\sin^2 \theta_{12}$ and $\sin^2 \theta_{13}$ and consider the bounds on these parameters from individual measurements. In sec. 6 the sensitivity of future, in particular, the low energy (LowNu) solar neutrino experiments to 1-3 mixing, is estimated. We discuss possible implications of future measurements of θ_{13} in sec 7. Our results are summarized in sec. 8.

2 The survival probability and θ_{13}

The analytic formula which describes conversion of the solar neutrinos in the case of three neutrino mixing and mass split hierarchy, $m_{13}^2 \ll m_{21}^2$, has been derived long time ago [28, 29]. Here m_{13}^2 and m_{21}^2 are the mass splits associated to 1-3 mixing and to the main channel of the solar neutrino conversion correspondingly. The formula was analyzed and further corrected recently [30, 31, 32].

In view of future precision measurements one needs to have an accurate formula for the probability with all relevant corrections included and errors due to approximation made estimated. For this reason we re-derive the formula in a simple and adequate way which employs features of the Large Mixing Angle (LMA) MSW solution. We will use a very high level of adiabaticity [34, 35, 36, 37] in whole 3 system.

Due to loss of coherence between the mass eigenstates, ν_i ($i=1,2,3$), the ν_e survival probability can be written as

$$P_{ee} = \sum_{i=1,2,3}^X P_{ei}^{\text{sun}} P_{ie}^{\text{Earth}}; \quad (8)$$

where P_{ei}^{sun} is the probability of $\nu_e \rightarrow \nu_i$ conversion in the Sun and P_{ie}^{Earth} is the $\nu_i \rightarrow \nu_e$ oscillation probability inside the Earth. Strong adiabaticity of the neutrino conversion in the Sun leads immediately to

$$P_{ei}^{\text{sun}} = |U_{ei}^{m0}|^2; \quad (9)$$

where U_{ei}^{m0} is the ei -element of neutrino mixing matrix in matter in the production point. $(U_{ei}^{m0})_{eh} = |j_{m_i}|$ determines the admixture of the eigenstates, ν_{m_i} , in the neutrino state in the initial point. Then due to adiabaticity ν_{m_i} transforms to ν_i when neutrino propagates to the surface of the Sun). Corrections due to non-adiabaticity, are negligible [37].

Combining (8) and (9) we obtain

$$P_{ee} = \sum_{i=1,2,3} U_{ei}^{m0} U_{ie}^{E\text{arth}} P_{ie}^{E\text{arth}} \quad (10)$$

In the absence of the Earth matter effect (the day signal) we have

$$P_{ie}^{E\text{arth}} = U_{ei}^2 \quad (11)$$

where U_{ei} are the elements of the vacuum mixing matrix.

In what follows we will neglect the Earth matter effect on the 1-3 mixing which is determined by $2E V_E = m_{13}^2 < 0.005$, (here V_E is the typical potential inside the Earth). Therefore

$$P_{3e}^{E\text{arth}} = U_{e3}^2 \quad (12)$$

The Earth matter effect on two other probabilities can be described by the term F_{reg} defined as the deviation from the no-oscillation case:

$$P_{2e}^{E\text{arth}} = U_{e2}^2 + F_{\text{reg}} \quad (13)$$

Then the unitarity condition, $\sum_{i=1,2,3} P_{ie}^{E\text{arth}} = 1$ and (12) lead to

$$P_{1e}^{E\text{arth}} = U_{e1}^2 - F_{\text{reg}} \quad (14)$$

Plugging (11, 12, 14) into (10) we obtain

$$P_{ee} = \sum_{i=1,2,3} U_{ei}^{m0} U_{ei}^2 + F_{\text{reg}} U_{e2}^{m0} U_{e1}^{m0} \quad (15)$$

We will use the standard parameterization of the mixing matrix in terms of mixing angles:

$$U_{e1} = \cos \theta_{13} \cos \theta_{12}; \quad U_{e2} = \cos \theta_{13} \sin \theta_{12}; \quad U_{e3} = \sin \theta_{13}; \quad (16)$$

and similar definition holds for the matrix elements in matter with substitution $\theta_{13} \rightarrow \theta_{13}^{m0}$ and $\theta_{12} \rightarrow \theta_{12}^{m0}$. The angle θ_{12} is identified with the "solar mixing angle".

In terms of mixing angles the probability (15) can be rewritten as

$$P_{ee} = \cos^2 \theta_{13}^{m0} \cos^2 \theta_{13} P_{ad} + \sin^2 \theta_{13}^{m0} \sin^2 \theta_{13} - F_{\text{reg}} \cos^2 \theta_{13}^{m0} \cos 2\theta_{12}^{m0}; \quad (17)$$

where P_{ad} is the usual two neutrino adiabatic probability:

$$P_{ad} = \sin^2 \theta_{12} + \cos^2 \theta_{12}^{m0} \cos 2\theta_{12}; \quad (18)$$

For $F_{\text{reg}} = 0$ the probability (17) coincides with the one found in [29].

Let us find the mixing angle θ_{13}^{m0} in matter. The Hamiltonian of 3 system can be written in the flavor basis as

$$H = U_{23} U_{13} U_{12} H^d U_{12}^y U_{13}^y U_{23}^y + V_3 \quad (19)$$

Here $H^d = \text{diag}(0; m_{21}^2=2E; m_{13}^2=2E)$, $V_3 = \text{diag}(V; 0; 0)$, and $V = \frac{P}{2G_F} Y_e$, where P is the matter density and Y_e is the electron number density fraction.

Performing rotations $U_{23}U_{13}$ we arrive at the basis $(\frac{0}{e}; \frac{0}{2}; \frac{0}{3})$ in which the Hamiltonian becomes

$$H = U_{12}H^dU_{12}^y + U_{13}^yVU_{13} \quad (20)$$

If the matter effect is small we can neglect mixing of the third state (off-diagonal terms of the matrix $U_{13}^yVU_{13}$). This state then decouples and for the rest of the system the Hamiltonian becomes

$$H_2 = U_{12}H^dU_{12}^y + \cos^2 \theta_{13}V_2 \quad (21)$$

where $V_2 = \text{diag}(V; 0)$.

In the lowest approximation the matter effect on the 1-3 mixing can be found making an additional 1-3 rotation which eliminates the 1-3 elements in (20). The angle of rotation, θ_{13}^0 , is given by

$$\tan 2\theta_{13}^0 = \frac{V \sin 2\theta_{13}}{m_{13}^2=(2E) - V \cos 2\theta_{13} + m_{21}^2=(2E) \sin^2 \theta_{12}} \sin 2\theta_{13} \quad (22)$$

where

$$\theta_{13}^0 = \frac{2EV}{m_{13}^2} = 0.062 \frac{E}{10M eV} \frac{Y_e}{100g=cc} \frac{2.5 \cdot 10^3 eV^2}{m_{13}^2} \quad (23)$$

So, approximately, $\theta_{13}^0 = \theta_{13}$.

The additional 1-3 rotation generates negligible 2-3 elements¹

$$H_{23} = \frac{V}{4} \sin 2\theta_{13} \sin 2\theta_{12} \frac{m_{21}^2}{m_{13}^2} \quad (24)$$

It also leads to corrections to the 1-2 block of the Hamiltonian:

$$H_2 = U_{12}H^dU_{12}^y + \cos^2 \theta_{13} \sin^2 \theta_{13} V_2 \quad (25)$$

In the first order in $2VE = m_{13}^2$ the rotation θ_{13}^0 decouples the third state. So, the 1-3 mixing angle in matter is given by

$$\theta_{13}^m = \theta_{13}^0 + \theta_{13} + O(\theta_{13}^0 \theta_{13}) \quad (26)$$

and using (22) we obtain

$$\sin^2 \theta_{13}^m = \sin^2 \theta_{13} (1 + 2\theta_{13}^0) + O(\theta_{13}^0 \sin^2 \theta_{13}); \sin^4 \theta_{13} \theta_{13}^0 \quad (27)$$

(See also [30].) For typical energy $E = 10 M eV$ the relative matter correction is (10-15)%. The correction is negligible at low energies.

¹Elimination of this term requires an additional 2-3 rotation by the angle $\theta_{23}^0 = 2EH_{23} = m_{21}^2 < 10^{-4}$.

The 1-2 mixing in matter is determined from diagonalization of (21) or (25) which means that neglecting very small correction ($\propto \sin^2 \theta_{13}$) in (25) one needs to use for m_{12} the standard 2 formula with substitution $V \rightarrow V \cos^2 \theta_{13}$.

Let us find dependence of F_{reg} , which describes the oscillation effect in the matter of the Earth, on the 1-3 mixing explicitly. The probability of $\nu_e \rightarrow \nu_e$ conversion can be written in terms of the amplitudes of transitions between the mass states ν_1, ν_2 , A_{12} , as

$$P_{2e} = |A_{12}U_{e1} + A_{22}U_{e2}|^2 = \cos^2 \theta_{13} |A_{12} \cos \theta_{12} + A_{22} \sin \theta_{12}|^2 \quad (28)$$

Since in the absence of the matter effect $A_{12} = 0$ and $A_{22} = 1$, in the lowest approximation in A_{12} / V , we obtain

$$F_{reg} = \cos^2 \theta_{13} \sin^2 2\theta_{12} \text{Re} A_{12} \quad (29)$$

The transition amplitude A_{12} should be found by the solution of the evolution equation with the Hamiltonian (25). It is proportional to the potential: $A_{12} / V \cos^2 \theta_{13}$, and consequently, F_{reg} (29) can be rewritten as

$$F_{reg} = \cos^4 \theta_{13} f_{reg} + O(f_{reg}^2); \quad (30)$$

where

$$f_{reg} = \sin^2 2\theta_{12} \text{Re} A_{12}^0 \quad (31)$$

is the ν_e regeneration factor calculated with 2 amplitude $A_{12}^0 = A_{12} = \cos^2 \theta_{13}$, and it does not depend on θ_{13} .

The regeneration factor integrated with the exposure function over the zenith angle can be estimated as

$$f_{reg} = \frac{E V_0 \sin^2 2\theta_{12}}{4 m_{21}^2}; \quad (32)$$

where V_0 is the potential at the surface of the Earth.

Inserting the expression for F_{reg} into (17) we obtain

$$P_{ee} = \cos^2 \theta_{13} \cos^2 \theta_{13} (P_{ad} \cos^2 \theta_{13} \cos^2 2\theta_{12} f_{reg}) + \sin^2 \theta_{13} \sin^2 \theta_{13} \quad (33)$$

Taking the mixing angle θ_{13} in the first order in θ_{13} we find

$$P_{ee} = \cos^4 \theta_{13} (1 - 2 \tan^2 \theta_{13}) (P_{ad} \cos^2 \theta_{13} \cos^2 2\theta_{12} f_{reg}) + \sin^4 \theta_{13} \quad (34)$$

Notice that the pre-factor $(1 - 2 \tan^2 \theta_{13})$ which describes the matter effect on the 1-3 mixing differs in the high and low energy limits.

The expression (33) can be rewritten as

$$P_{ee} = \cos^2 \theta_{13} \cos^2 \theta_{13} P_{ee}^{(2)}(\theta_{12}; \theta_{13}) + \sin^2 \theta_{13} \sin^2 \theta_{13}; \quad (35)$$

where

$$P_{ee}^{(2)} = P_{ad} \cos^2 \theta_{13} \cos^2 \theta_{12} f_{reg}$$

is the total ν_e survival probability for two-neutrino mixing which includes both the conversion in the Sun and oscillations in the Earth. P_{ad} depends on θ_{13} via the effective matter potential $V \cos^2 \theta_{13}$.

The probability should be averaged over the distribution of the neutrino sources in the Sun. For the K -component of the solar neutrino spectrum ($K = pp; Be; pep; B; N; O$) the averaged probability can be written as [37]

$$P_{ee;K}^{(2)} = \sin^2 \theta_{13} + \cos^2 \theta_{13} (V_K) \cos^2 \theta_{12} \cos^2 \theta_{13} f_{reg}; \quad (36)$$

where V_K is the effective value of the matter potential in the region of production of the K neutrino component. θ_K is an additional correction due to the integration over the production region [37], and in what follows we will neglect it.

Notice there are three features of dynamics of propagation which allow one to immediately derive the 3 survival probability in terms of the 2 probabilities in a general context:

- 1). A diabaticity of propagation of the third neutrino;
- 2). Negligible Earth matter effect on 1-3 mixing;
- 3). A veraging of oscillations/loss of coherence of the third mass eigenstate.

Essentially this means that the third neutrino eigenstate decouples from dynamics and propagates independently. Its contribution to the probability adds incoherently. Therefore the problem is reduced to two neutrino problem and additional factors in (33) are just projection of the flavor basis onto the basis of states which contains the decoupling state ν_{3m} . In (35) factors $\sin^2 \theta_{13}^{m0}$ and $\cos^2 \theta_{13}^{m0}$ are from the projection in the initial state, whereas the factors $\sin^2 \theta_{13}$ and $\cos^2 \theta_{13}$ are from projection in the final state.

Up to negligible corrections the expression for the probability (35) can be rewritten in form

$$P_{ee} = (1 - \sin^2 \tilde{\theta}_{13})^2 P_{ee}^{(2)}(\theta_{12}; \tilde{\theta}_{13}) + \sin^4 \tilde{\theta}_{13}; \quad (37)$$

where

$$\sin^2 \tilde{\theta}_{13} = \sin^2 \theta_{13} (1 + \theta_{13}^2); \quad (38)$$

which coincides with the form without matter corrections to θ_{13}^2 . This means that the matter effect on the 1-3 mixing in the probability can be accounted by renormalization of $\sin^2 \theta_{13}$. Inversely, using usual formula for the probability without matter corrections in the analysis of the

²Strictly, this is correct in the high energy or low energy limits, where $P_{ee}^{(2)} = P_{ad}$ depends very weakly on the potential. At low energies the matter corrections are negligible anyway (see sec. 2).

data we determine $\tilde{\theta}_{13}$ averaged over the relevant energy interval. Then the true vacuum mixing angle will be smaller:

$$\sin^2 \theta_{13} = \sin^2 \tilde{\theta}_{13} (1 - \delta_{13}) \quad (39)$$

Here $\delta_{13} = \frac{h_{13}^E}{E}$ is the value averaged over the relevant energy range. Renormalization depends on the neutrino energy: $\delta_{13} \approx 0.05$ at high energies and $\delta_{13} \approx 0.002$ in the pp-neutrino range, and the latter can be neglected.

3 Two limits

As we will see, the expected sensitivity of solar neutrino studies to the 1-3 mixing will not be better than $(\sin^2 \theta_{13}) \approx 0.01$. According to (35) that would correspond to the change of the survival probability

$$P \approx 2P (\sin^2 \theta_{13}) \approx 1\% \quad (40)$$

Therefore we can neglect in the present discussions various corrections to the probability which are much smaller than 0.01. In particular,

The term $\sin^4 \theta_{13} < 0.002$ can be neglected in eq. (35).

The matter effect on the 1-3 mixing is small and can be taken into account as a small renormalization of $\sin^2 \theta_{13}$ (see sec. 2).

We will neglect $f_{\text{reg}} < 10^{-3}$ corrections in F_{reg} .

In qualitative consideration we will use simplified expressions for the survival probability obtained in the limits of high and low energies. In fact, all relevant fluxes are either in the low (pp; Be; N; O; pep) or in the high, $E > 5 \text{ MeV}$ (B, hep), energy limits. The expansion parameter equals

$$\frac{m_{21}^2}{2EV} \quad (41)$$

at high energies and $1 = \dots$ at low energies³.

1). In the high energy limit, performing expansion of (36) in \dots we find the survival probability

$$P_{ee}^{(h)} \approx \cos^4 \theta_{13} \sin^2 \theta_{12} + \frac{1}{4} \cos^2 \theta_{12} \sin^2 2\theta_{12} + \cos^6 \theta_{13} f_{\text{reg}} \quad (42)$$

Here the first term is due to the non-oscillatory adiabatic conversion. In the second term, which describes the effect of averaged oscillations, dependence on θ_{13} is absent. In contrast, the third

³Notice that in [37] we use different definition of \dots : $\dots = \dots$.

(regeneration) term has the strongest dependence on θ_{13} [32]. It originates from the common factor $\cos^4 \theta_{13}$ and the effective potential in the 3 case which contains another $\cos^2 \theta_{13}$ factor.

In the lowest order in $\sin^2 \theta_{13}$ we can rewrite (42) as

$$P_{ee}^{(h)} = \sin^2 \theta_{12} + \frac{1}{4} \cos 2\theta_{12} \sin^2 2\theta_{12} + f_{\text{reg}} \sin^2 \theta_{13} (2 \sin^2 \theta_{12} + 3f_{\text{reg}}): \quad (43)$$

Neglecting the oscillation corrections (second term) and the double suppressed term $\sin^2 \theta_{13} f_{\text{reg}}$ we obtain

$$P_{ee}^{(h)} = (1 - 2 \sin^2 \theta_{13}) \sin^2 \theta_{12} + f_{\text{reg}}: \quad (44)$$

2). For the low energy neutrinos ($E < 2 \text{ M eV}$), the matter effect is small and in the lowest order in $1/E$ we have

$$P_{ee}^{(l)} = \cos^4 \theta_{13} (1 - 0.5 \sin^2 2\theta_{12}) - 0.5 \cos^6 \theta_{13} \cos 2\theta_{12} \sin^2 2\theta_{12} + \dots: \quad (45)$$

Here the first term is the effect of averaged vacuum oscillations. The second one gives the matter effect correction which contains strong dependence on θ_{13} . An additional second power of $\cos \theta_{13}$ originates from the matter potential. The regeneration effect is neglected. Numerical calculations confirm that the linear in $1/E$ approximation (45) works well up to 2 M eV .

In the lowest order in $\sin^2 \theta_{13}$ we find from (45)

$$P_{ee}^{(l)} = 1 - \frac{1}{2} \sin^2 2\theta_{12} - 0.5 \cos 2\theta_{12} \sin^2 2\theta_{12} + \dots: \quad (46)$$

$$\sin^2 \theta_{13} (2 - \sin^2 2\theta_{12} - 1.5 \cos 2\theta_{12} \sin^2 2\theta_{12}) + \dots: \quad (47)$$

For very low energies (pp-range) the matter corrections can be neglected, so that

$$P_{ee}^{(l)} = (1 - 2 \sin^2 \theta_{13}) (1 - 0.5 \sin^2 2\theta_{12}): \quad (48)$$

According to Eqs. (42 - 47),

The dependences of the probability on θ_{12} for the high energies and low energies are opposite: $P_{ee}^{(l)}$ increases, whereas $P_{ee}^{(h)}$ decreases with decrease of θ_{12} .

In contrast, $P_{ee}^{(l)}$ and $P_{ee}^{(h)}$ both decrease with increase of θ_{13} . So, θ_{12} and θ_{13} correlate at low energies and anti-correlate at high energies. For the ^8B neutrinos an increase of θ_{13} can be compensated by increase of θ_{12} , whereas at low energies (for the pp neutrinos), θ_{12} should decrease to compensate increase of θ_{13} .

Both for the high and low neutrino energies dependence of the probability on m_{21}^2 appears via small corrections only, and therefore, is weak.

Apparently strong dependence on θ_{13} cancels if the ratio of probabilities (or the ratio of the corresponding observables) is considered:

$$\frac{P_{ee}^{(h)}}{P_{ee}^{(l)}} = \frac{\sin^2 \theta_{12} + 0.25 \cos^4 \theta_{13} \cos 2\theta_{12} \sin^2 2\theta_{12} + \cos^2 \theta_{13} f_{\text{reg}}}{1 - 0.5 \sin^2 2\theta_{12}} \quad (49)$$

Notice that dependence of the ratio on θ_{13} appears in small corrections and it can be neglected in the first approximation. So, measurements of the ratio gives $\sin^2 \theta_{12}$. Then one of the probabilities (in low or high limits) can be used to find $\sin^2 \theta_{13}$.

4 $\sin^2 \theta_{12}$ - $\sin^2 \theta_{13}$ plots and iso-contours of observables

There are two important features of the problem:

- Weak dependence of the probability and observables on m_{21}^2 within the allowed region;
- $\sin^2 \theta_{12}$ - $\sin^2 \theta_{13}$ degeneracy.

Let us consider these features in some details.

1). The KamLAND spectral data has shown high precision in determination of m_{21}^2 . The relative error

$$\frac{(\delta m_{21}^2)}{m_{21}^2} \quad (50)$$

is about $\approx 12\%$ [3] at the present, and with 3 kTyr statistics from KamLAND this can further reduce to 7% [38].

As follows from (42) and (47), variation of the probability in the high energy limit with m_{21}^2 equals:

$$P_{ee}^{(h)} = \frac{1}{2} \cos^2 \theta_{12} \sin^2 2\theta_{12} \cos^6 \theta_{13} f_{\text{reg}} \quad (51)$$

For $E = 10$ MeV and $\theta_{13} = 0.1$, we find $P_{ee} = 0.005$.

In the low energy part, variations of the probability with m_{21}^2 are even weaker:

$$P_{ee}^{(l)} = \frac{1}{2} \cos^6 \theta_{13} \cos 2\theta_{12} \sin^2 2\theta_{12} \quad (52)$$

For $E = 0.4$ MeV we find $P_{ee}^{(3)} = 0.011 - 0.001$.

2). According to the discussion in sec. 2, in the first approximation, experiments which probe the high energy part of the spectrum are sensitive to the same combination of mixing angles θ_{12} and θ_{13} . Similar statement is true for the low energy experiments but the combination of mixing

angles is different. Therefore to determine \sin^2_{12} and \sin^2_{13} separately one needs to employ both types of experiments.

In view of these two features, we will present results of our study in \sin^2_{12} - \sin^2_{13} plane for fixed values of m^2_{21} .

Let us construct the contours of constant values of various observables in the \sin^2_{12} - \sin^2_{13} plane. Essentially, the iso-contours for a given observable X coincide with the contours of constant survival probability averaged over the relevant energy range with the corresponding cross-section:

$$\langle R_{ee} \rangle_X = C_X : \quad (53)$$

The survival probabilities found in the high and low energy limits determine two different types of the iso-contours. For the high energy observables ($E > 5$ MeV), using Eq. (43), we find an analytic expression for the contours of constant X :

$$\sin^2_{13} = \frac{\sin^2_{12} + 0.25 \cos 2\theta_{12} \sin^2 2\theta_{12} \frac{m^2_{21}}{X} + \langle R_{reg} \rangle_X C_X}{2 \sin^2_{12} + 3 \langle R_{reg} \rangle_X} ; \quad (54)$$

where

$$\langle R_{reg} \rangle_X = \frac{m^2_{21}}{2E V_B} ; \quad (55)$$

is the averaged over the neutrino energy value of $\langle R \rangle$ folded with the cross-section, energy resolution of detector, etc.. In the allowed range of \sin^2_{12} (with the average value of θ_{12}) the strongest dependence comes from the denominator of (54):

$$\sin^2_{13} \approx A (\sin^2_{12} - C_X) ; \quad A = (2 \sin^2_{12} + 3 \langle R_{reg} \rangle)^{-1} ; \quad (56)$$

So, in the first approximation the contours are straight lines. This reproduces well the results of numerical calculations presented in sec. 5, 6. Notice that \sin^2_{13} increases with \sin^2_{12} .

For the low energy observables, using (47), we obtain expressions for the iso-contours of observable Y :

$$\sin^2_{13} = \frac{1 - 0.5 \sin^2 2\theta_{12} - 0.5 \cos 2\theta_{12} \sin^2 2\theta_{12} \frac{m^2_{21}}{Y}}{2 \sin^2 2\theta_{12} - 1.5 \cos 2\theta_{12} \sin^2 2\theta_{12} \frac{m^2_{21}}{Y}} ; \quad (57)$$

where

$$\frac{m^2_{21}}{Y} = \frac{2E V}{m^2_{21}} ; \quad (58)$$

In the rough approximation

$$\sin^2_{13} / (1 - C_Y) \approx 2 \sin^2_{12} (1 - \sin^2_{12}) \quad (59)$$

and it has minimum at $\sin^2_{12} = 0.5$. Other terms in (57) shift this minimum to smaller values of \sin^2_{12} . So, in the region of interest, $\sin^2_{12} \approx 0.3$, the lines of constant values of observables have negative slope: \sin^2_{13} decreases with \sin^2_{12} .

5 Constraints on the mixing parameters from the present experiments

In this section we describe the results of our numerical computations.

We first perform the global analysis of different data samples. Some details of the analysis follow. The χ^2 depends on m_{31}^2 and in our case we allow this parameter to vary freely in the range allowed by the zenith angle SuperKamokande atmospheric neutrino data [39]. The details of procedure for the solar and CHOOZ data can be found in [25] while the KamLAND analysis follows the method outlined in [26, 4]. We use the KamLAND data from Ref. [40].

For the solar neutrinos we include the data on total rates from the radiochemical experiments Cl [41] and Ga (SAGE, GALLEX and GNO combined) [42], the SuperKamokande day-night spectrum data [43], the SNO CC (charged current), ES (neutrino-electron scattering) and NC (neutral current) rates from the salt phase and the combined CC+ES+NC energy spectrum from the pure D₂O phase [44].

The ⁸B neutrino flux normalization, $f_B = F_B / F_B^{SSM}$, where F_B is the true flux and F_B^{SSM} is the flux predicted in the SSM [45], is left as a free parameter in the fit. Essentially f_B is fixed by the NC data from the SNO experiment. For the other flux normalizations and uncertainties we use the predictions from the Standard Solar Model (SSM) [45].

In Fig. 1 we show the allowed regions of the parameters $\sin^2 \theta_{12}$ - $\sin^2 \theta_{13}$ which follow from the global fit of all available solar neutrino data as well as data from reactor experiments KamLAND and CHOOZ. The global minimum has been obtained by letting all the parameters (including m_{21}^2) vary freely in the fit. Values of parameters in the global minimum come at ⁴

$$m_{21}^2 = 8.4 \cdot 10^5 \text{ eV}^2; \quad \sin^2 \theta_{12} = 0.28; \quad \sin^2 \theta_{13} = 0.00; \quad f_B = 0.89; \quad (60)$$

The two panels in Fig. 1 correspond to two fixed illustrative values of m_{21}^2 from the current allowed range. The contours are plotted with respect to the global minimum (60) using the definition of χ^2 which corresponds to 3 parameters. The upper bound, $\sin^2 \theta_{13} < 0.057$ (99% C.L.), is in agreement with results of other analyses [5, 3].

According to Fig. 1 with increase of m_{21}^2 the allowed region shifts to smaller $\sin^2 \theta_{12}$; with increase of $\sin^2 \theta_{13}$ the value of $\sin^2 \theta_{12}$ in minimum of χ^2 practically does not change.

We have performed the global fit of the solar neutrino data only. The best-fit values of parameters are found to be

$$m_{21}^2 = 6.1 \cdot 10^5 \text{ eV}^2; \quad \sin^2 \theta_{12} = 0.29; \quad \sin^2 \theta_{13} = 0.01; \quad f_B = 0.91; \quad (61)$$

Now the 1-3 mixing is non-zero.

This is in agreement with $\sin^2 \theta_{13} = 0.02$ obtained in [5]. Indeed, the solar χ^2 is quite flat in the region $\sin^2 \theta_{13} = 0 - 0.03$. For $\sin^2 \theta_{13} = 0.01$ and 0.02 we obtain the $m_{\text{min}}^2 = 68.78$ and 68.79 correspondingly.

⁴In the latest version of their paper [46] KamLAND collaboration has identified a new source of background. Including this, we get the best fit values $m_{21}^2 = 8 \cdot 10^5 \text{ eV}^2$; $\sin^2 \theta_{12} = 0.28$; $\sin^2 \theta_{13} = 0.004$; $f_B = 0.88$. This change does not influence results of our study of 1-3 mixing.

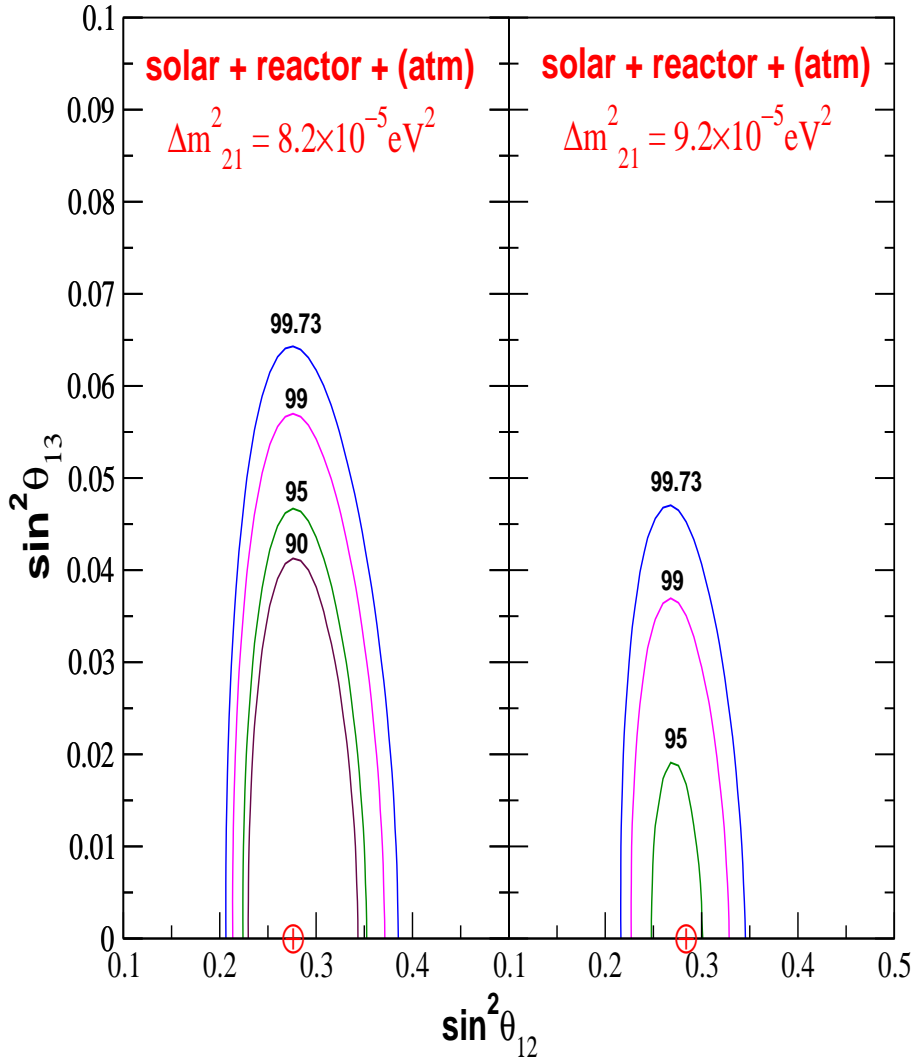


Figure 1: The 90% , 95% , 99% and 99.73% C.L. allowed regions of mixing angles from global χ^2 analysis of solar neutrino, KamLAND and CHOOZ neutrino data. The left panel is for $m^2_{21} = 8 \times 10^5 \text{ eV}^2$ and the right panel is for $m^2_{21} = 9 \times 10^5 \text{ eV}^2$. The global best-fit point obtained by letting all the parameters vary freely is marked by the crossed circle.

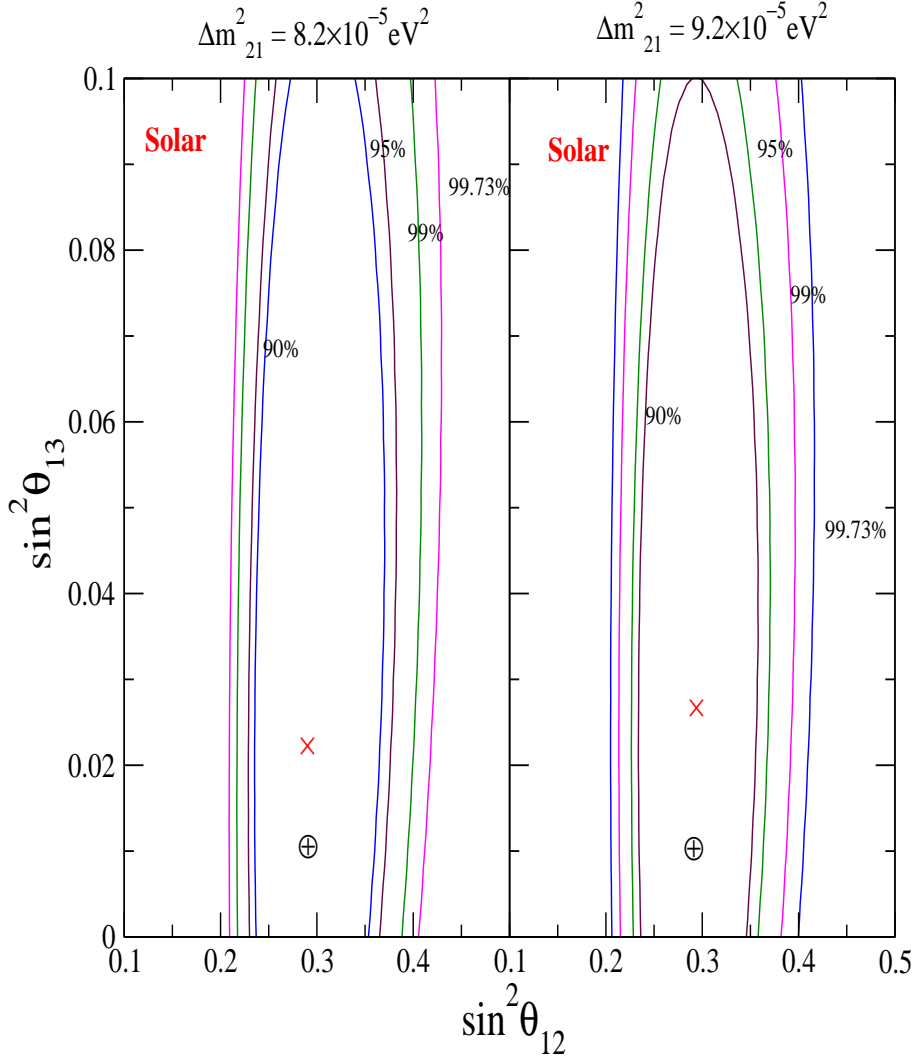


Figure 2: The 90% , 95% , 99% and 99.73% C.L. allowed regions of mixing angles from the global χ^2 analysis of solar neutrino data. The left panel is for $m_{21}^2 = 8 \times 10^5 \text{ eV}^2$ and the right panel is for $m_{21}^2 = 9 \times 10^5 \text{ eV}^2$. The global best-fit point obtained by letting all the parameters vary freely is marked by \oplus . Also shown by crosses are the local best-fit points obtained at fixed m_{21}^2 .

In Fig. 2 we show the contours obtained from global analysis of the solar neutrino data when m_{21}^2 is fixed. The constant χ^2 contours have been calculated with respect to the global minimum (61) and using the χ^2 values corresponding to 3 parameters. We also show the local minimum found for fixed values of m_{21}^2 . In particular, for $m_{21}^2 = 8 \cdot 10^6 \text{ eV}^2$ we obtain

$$\sin^2 \theta_{13} = 0.022^{+0.088}_{-0.022} \quad (90\% \text{ C.L.}) \quad (62)$$

The best value increases with m_{21}^2 and for $m_{21}^2 = 9 \cdot 10^6 \text{ eV}^2$ we find $\sin^2 \theta_{13} = 0.026$. The figure 2 shows also that at present solar data alone has a weak sensitivity to $\sin^2 \theta_{13}$: the 90% C.L. bound is $\sin^2 \theta_{13} < 0.11$.

Let us now consider bounds on mixing angles θ_{12} and θ_{13} from particular observables.

1). At present only the gallium experiments can be considered as the low energy experiments. For the G_e -production rate, Q_{G_e} , we can write

$$Q_{G_e} = \sum_i P_{ee}^{pp} Q_{G_e}^{pp} + P_{ee}^{pep} Q_{G_e}^{pep} + P_{ee}^{Be} Q_{G_e}^{Be} + P_{ee}^{CNO} Q_{G_e}^{CNO} + P_{ee}^B f_B Q_{G_e}^B \quad (63)$$

where $Q_{G_e}^i$ are the contributions to the rate from the i component of the solar neutrino flux according to the SSM, P_{ee}^i is the corresponding effective (averaged over the energy range) survival probabilities. The rate has the contributions both from the low and high energy parts of the spectrum, though the latter (from boron neutrinos) is much smaller. We can subtract the boron neutrino effect, $Q_{G_e}^{B \text{ exp}}$, using experimental results from SNO: $Q_{G_e}^1 = Q_{G_e} - Q_{G_e}^{B \text{ exp}}$. Taking the ^8B flux from SNO as an input, we find that the ^8B neutrino contribution equals $Q_{G_e}^{B \text{ exp}} = 4.2^{+1.4}_{-0.7}$ SNU and then $Q_{G_e}^1 = 63.9^{+5.1}_{-5.2}$ SNU for the rest of the neutrinos [42].

The conversion effect on $Q_{G_e}^1$ is described by the probability in low energy limit:

$$Q_{G_e}^1 = (Q_{G_e}^{SSM} - Q_{G_e}^{B \text{ exp}}) \cos^4 \theta_{13} (1 - 0.5 \sin^2 2\theta_{12}) \cos^2 \theta_{13} \cos 2\theta_{12} \sin^2 2\theta_{12} \quad (64)$$

where

$$\frac{1}{Q_{G_e}^1} = \frac{1}{Q_{G_e}^{SSM} - Q_{G_e}^{B \text{ exp}}} \left(\frac{1}{\cos^4 \theta_{13}} + \frac{1}{\cos^2 \theta_{13} \cos 2\theta_{12} \sin^2 2\theta_{12}} \right) \quad (65)$$

Results of numerical calculations are given in Figs. 3, 4, 5, where we show the contours of constant rate Q_{G_e} which correspond to the present central value as well as to 1 and 2 deviations from it. (The contours are well described by the analytical expression given in (57) with $Y^1 = Q_{G_e}^1$ and $C_Y = C_{G_e}$.)

For zero $1-3\sigma$ mixing the central value of $Q_{G_e} = 68.1$ SNU corresponds to $\sin^2 \theta_{12} = 0.34$, and the best fit value $\sin^2 \theta_{12} = 0.28$ is accepted at 1 σ level. For a given Q_{G_e} , $\sin^2 \theta_{13}$ increases with decrease of $\sin^2 \theta_{12}$. Taking the best fit value $\sin^2 \theta_{12} = 0.29$ (61) and $Q_{G_e} = 68.1$ SNU we find $\sin^2 \theta_{13} = 0.03$.

2). The CC/NC ratio of events at SNO is given by the integrated (with cross-section) survival probability at high energies: $CC/NC = h P_{ee}^{(h)}$. The iso-contours are described approximately by Eq. (54) with $C_X = C_{SNO} = CC/NC$. The results of exact numerical calculations are shown in

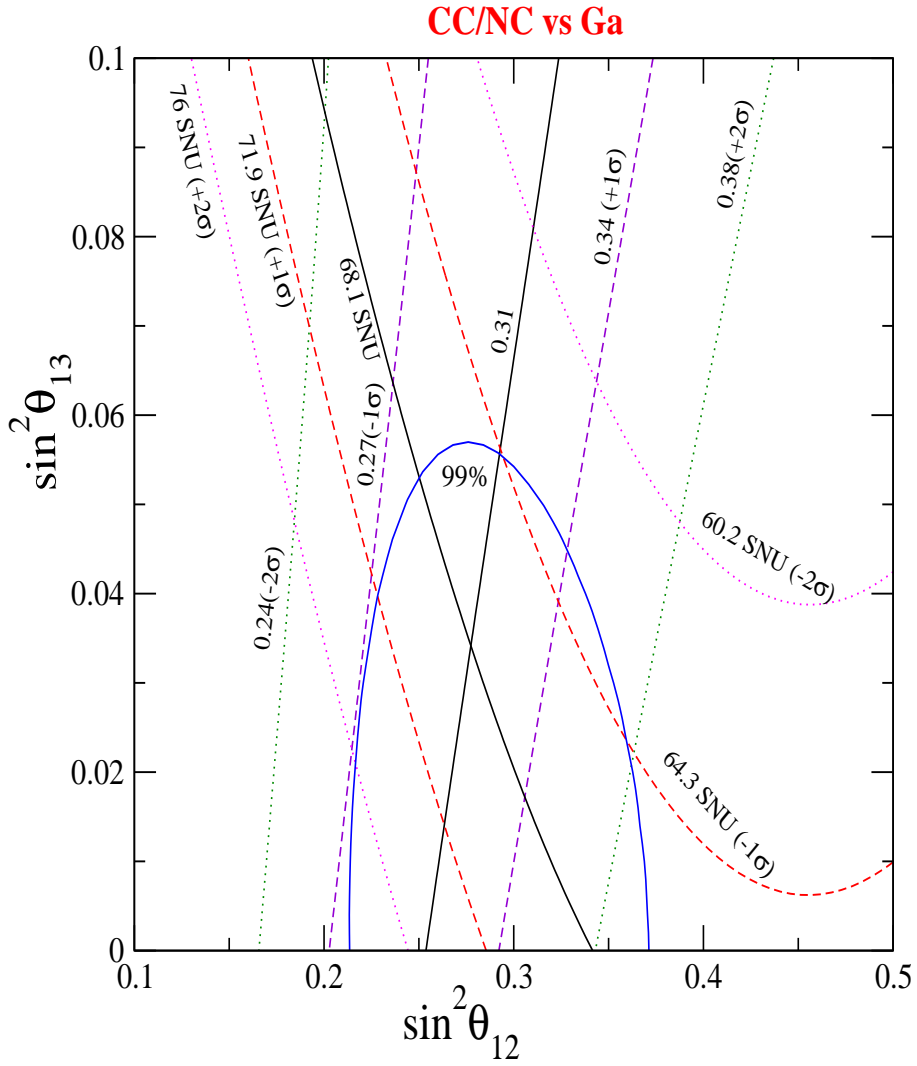


Figure 3: The iso-contours of the CC/NC ratio at SNO and Ge-production rate in the $\sin^2 \theta_{12}$ $\sin^2 \theta_{13}$ plane for $m_{21}^2 = 8 - 10^6 \text{ eV}^2$. Shown are the iso-contours for the central values of observables and the 1 and 2 deviations. The solid (blue) contour restricts the 99% C.L. allowed area from the global fit of all data.

g. 3. The iso-contours are constructed for the present central value of CC/NC as well as for its 1 and 2 deviations. At $\sin^2_{12} = 0.29$ the central value of CC/NC gives $\sin^2_{13} = 0.04$.

As seen from g. 3, the combination of SNO CC/NC and Ga-results prefers the non-zero 1-3 mixing. The iso-contours of the central observed values of CC/NC and Q_{Ge} cross at

$$\sin^2_{13} = 0.034 \quad 0.026 \quad (66)$$

which is about 1.3 deviation from zero. Here \sin^2_{13} is evaluated from the g.3 using CC/NC and Q_{Ge} measurements. The value (66) deviates by 2.2 if \sin^2_{13} is taken from the global fit (2).

The CC/NC ratio is free of the 8B neutrino normalization factor f_B . Iso-contours for the of Ga-production rate are constructed for $f_B = 1$, i.e., for the SSM value of the 8B flux. The dependence of Q_{Ar} on f_B essentially disappears if one uses for the boron neutrino flux the value measured by NC in SNO or by SK. In any case the influence of uncertainty related to f_B on the intersection of iso-contours is weak. Larger uncertainty (~ 1 SNU) follows from the Be-neutrino flux contribution. That leads to $\sin^2_{13} \sim 0.01$. Future Borexino measurements can reduce this uncertainty.

3). The SuperK annual rate of the $\bar{\nu}_e$ events. The ratio of the observed to SSM predicted event rates is given by

$$R_{SK} = f_B [\rho_{eei}(1 - r) + r]; \quad (67)$$

where $r = \frac{\sigma_{\nu_e e}}{\sigma_{\nu_e \bar{\nu}_e}}$ is the ratio of the $\nu_e e$ and $\nu_e \bar{\nu}_e$ cross-sections. The lines of constant R_{SK} coincide with the lines of constant $\rho_{eei} = C_{SK}$, where according to (67)

$$C_{SK} = \frac{R_{SK} - f_B r}{1 - r}; \quad (68)$$

The lines are given by the Eq. (54) with $C_X = C_{SK}$ and the averaging (integration) $\langle \dots \rangle_X$ should be done according to the SK experiment characteristics.

The iso-contours of the SK rate in the $\sin^2_{12} - \sin^2_{13}$ plane are presented in g. 4 for $f_B = 1$. They correspond to the SK central value $R_{SK} = 0.41$ as well as the 1 and 2 deviations. According to g. 4, for $\sin^2_{13} = 0$ the ratio $R_{SK} = 0.41$ is achieved at $\sin^2_{12} = 0.21$ which is about 2 below the best global value. In turn, the best global value $\sin^2_{12} = 0.29$ and $R_{SK} = 0.41$ lead to $\sin^2_{13} = 0.1$.

With decrease of f_B the corresponding iso-contours shift to larger \sin^2_{12} and smaller \sin^2_{13} . For arbitrary f_B one can use the grid of contours calculated for $f_B = 1, R_{SK}^{(1)}$. Indeed, according to (68), for given values R_{SK} and f_B one should take the contour $R_{SK}^{(1)} = R_{SK} / f_B$.

The combination of SK - and Ga - data (crossing point of the contours which correspond to the central experimental values) selects $\sin^2_{13} = 0.053$ as is seen from g. 4. For $f_B = 0.9$ the best fit SK value $R_{SK} = 0.41$ corresponds to the iso-contour with $R_{SK}^{(1)} = 0.455$. The intersection of this contour with the iso-contour $Q_{Ge} = 68.1$ SNU occurs at much smaller 1-3 mixing: $\sin^2_{13} = 0.006$ and $\sin^2_{12} = 0.33$.

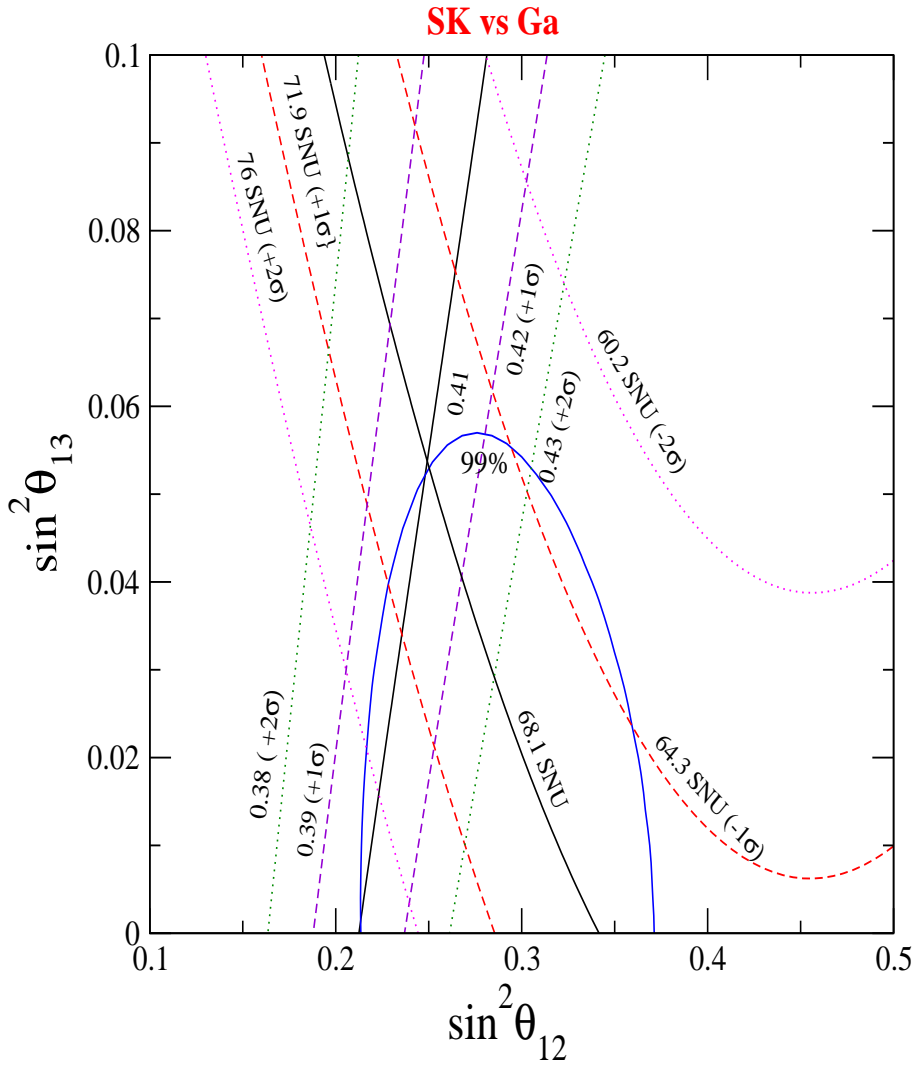


Figure 4: The iso-contours of R_{SK} and G -production rate in the $\sin^2 \theta_{12}$ - $\sin^2 \theta_{13}$ plane for $m_{21}^2 = 8 - 10^6 \text{ eV}^2$. Shown are the contours for the central values and $\pm 1, 2$ deviations from these central values. The solid (blue) contour restricts the 99% C.L. allowed area from the global fit of all data.

4). The Argon production rate in the Homestake experiment is determined by

$$Q_{Ar} = P_{ee}^h Q_{Ar}^{Be} + P_{ee}^{pep} Q_{Ar}^{pep} + P_{ee}^{CNO} Q_{Ar}^{CNO} + P_{ee}^B f_B Q_{Ar}^i \quad (69)$$

According to the SSM Q_{Ar} is dominated by the high energy (boron) neutrinos. Therefore the contours of constant rate (Fig. 5) have typical slope of the high energy observables. We show these contours for $f_B = 1$.

For $\sin^2_{13} = 0$ and the best global value of \sin^2_{12} the rate is about 3.15 SNU which is 2.5 above the experimental result. The combination of Cl and Ga results prefers large θ_{13} : $\sin^2_{13} = 0.1$ which deviates from zero by 2.5.

For the arbitrary f_B one needs to rescale Q_{Ar}^B : $Q_{Ar}^B = f_B Q_{Ar}^B$. Thus, for $f_B = 0.9$ and $Q_{Ar} = 2.55$ SNU the iso-contour with $Q_{Ar} = 3$ SNU should be used. It intersects with iso-contour $CC/NC = 0.31$ at $\sin^2_{13} = 0.05$.

Summarizing, all three possible combinations of the low and high energy experiments prefer non-zero value of \sin^2_{13} . For $m_{21}^2 = 8 \cdot 10^5 \text{ eV}^2$, the combination of SNO and Ga data selects $\sin^2_{13} = 0.034$, which is practically independent of f_B . The combination of SK and Ga results leads to $\sin^2_{13} = 0.006$ for $f_B = 0.9$. The combination of Cl and Ga data selects $\sin^2_{13} = 0.05$ at $f_B = 0.9$, however statistical significance of this result is lower. The average from these three combinations is about $\sin^2_{13} = 0.02$. It agrees very well with results of fit of all the solar data for the same m_{21}^2 : $\sin^2_{13} = 0.022$.

Notice that available spectral information does not give strong restriction on \sin^2_{13} . In fact, the flatness of the measured spectrum of events at SNO and SK may even favor non-zero \sin^2_{13} . Indeed, at high energies an increase of \sin^2_{13} implies increase of \sin^2_{12} and therefore flattening of the spectrum.

The results on θ_{13} described above are in agreement with the best fit value from the global analysis of all solar neutrino data, $\sin^2_{13} = 0.01$, which is realized, however, for smaller m_{21}^2 (61). Inclusion of the result from CHOOZ diminishes \sin^2_{13} to practically zero.

Let us consider dependence of the iso-contours on m_{21}^2 . Using (54) we find for the high energy part:

$$(\sin^2_{13}) = \frac{1}{2} \sin^2_{13} + \frac{C_X \sin^2_{12} - 3h_{reg}^i (0.5 \sin^2_{13})}{\sin^2_{12} + 1.5h_{reg}^i} \quad ; \quad (70)$$

where we have expressed \sin^2_{12} in terms of \sin^2_{13} .

In the low energy region according to (57)

$$(\sin^2_{13}) = \frac{1}{4} \frac{\cos^2_{12} \sin^2_{12}}{1 - 0.5 \sin^2_{12}} \quad ; \quad (71)$$

and the pre-factor is small: $(\sin^2_{13}) = 0.011$.

In Fig. 6 we show results of numerical calculations of the iso-contours for Ga-rate and CC/NC ratio for three different values of m_{21}^2 . In agreement with our qualitative consideration a shift of

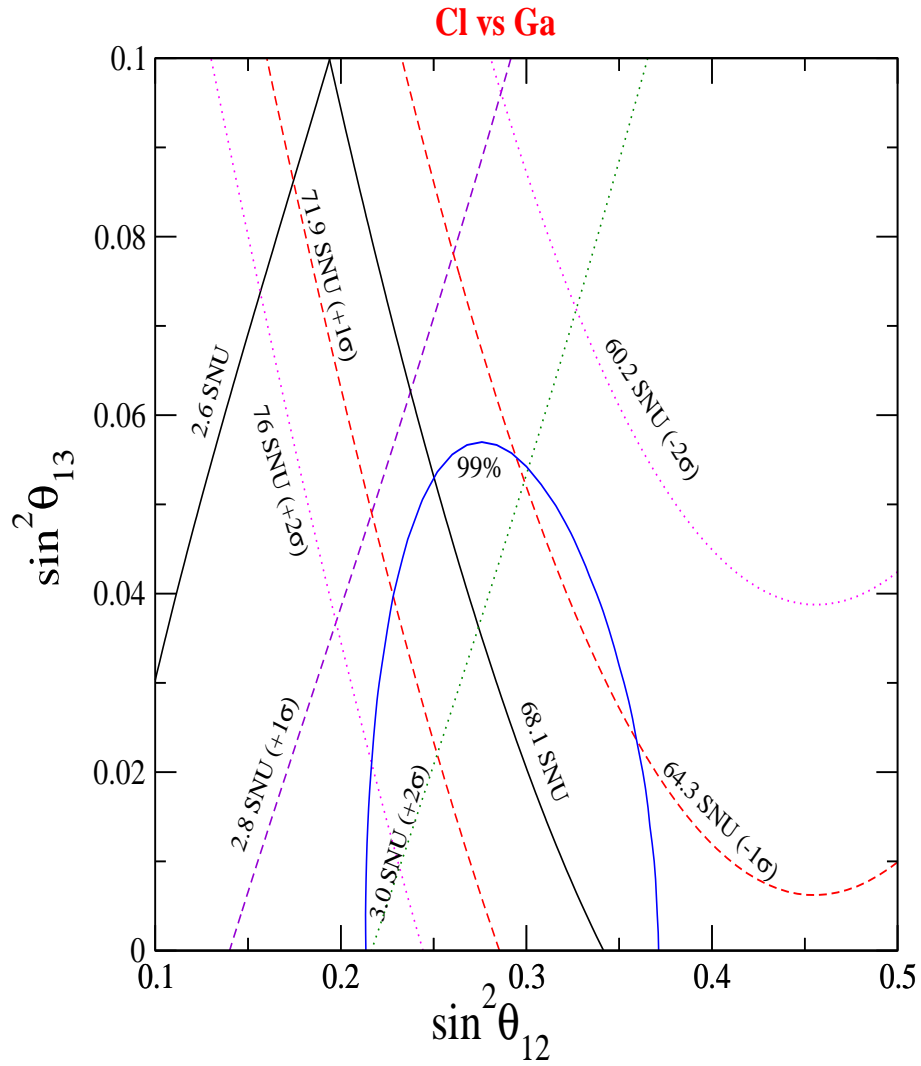


Figure 5: The iso-contours of the Ar- and Ge-production rates in the $\sin^2 \theta_{12}$ - $\sin^2 \theta_{13}$ plane for $m_{21}^2 = 8 \cdot 10^6 \text{ eV}^2$. Shown are the contours for the central values as well as ± 1 and ± 2 deviations. The contours are calculated for $f_B = 1$. The solid line restricts the 99% C.L. allowed area from the global fit of all data.

the low energy contours is much weaker. Variations of m_{21}^2 from 7 to $9 \times 10^5 \text{ eV}^2$ (which is about 25 % change) gives $(\sin^2_{13}) = 0.008$ and $(\sin^2_{12}) = 0.012$. Reduction of the uncertainty in m_{21}^2 down to 14% will result in $(\sin^2_{13}) = 0.004$ and $(\sin^2_{12}) = 0.007$. This is much smaller than the expected sensitivity of future solar neutrino studies.

Let us consider the effects of matter corrections to the 1-3 mixing. As we have established in sec. 2, the effect is reduced to renormalization of \sin^2_{13} according to Eq. (39). True value of \sin^2_{13} is smaller than extracted from the data without taking into account matter correction. The renormalization is negligible for the low energy observables and it is of the order 5% at high energies. So, the iso-contours of high energy observables should be shifted down by factor 0.95. This, in turn leads to decrease of \sin^2_{13} in the intersection points: e.g., instead of $\sin^2_{13} = 0.340$ one finds 0.327.

The figures presented in this section allow us to estimate relevance of the non-zero 1-3 mixing for the solar neutrino studies.

For a given CC/NC ratio an increase of \sin^2_{13} from 0 to 0.05 (3 upperbound) corresponds to decrease the Gallium rate by 2 or $Q_{Ge} \approx 8 \text{ SNU}$. Inversely, for a given Q_{Ge} , the same increase of \sin^2_{13} leads to 1.8 decrease of the ratio CC/NC: $CC/NC \approx 0.05$. For the same change of \sin^2_{13} the SK rate decreases by 4: $R_{SK} = 0.04$. So, the 1% variations of \sin^2_{13} produce about 1% or smaller variations of observables. This shows that \sin^2_{13} is relevant already for the present analysis of the solar neutrino data.

6 Sensitivity of the future solar neutrino experiments to 1-3 mixing

At present, some sensitivity of the solar neutrino data to the 1-3 mixing appears essentially due to the combination of the SNO - and SK - results from the one hand side and the Gallium experiment results from the other side. Future high precision measurements will have better sensitivity. To evaluate this sensitivity and to study possible implications of measurements we have constructed the grids of the iso-contours of various observables.

1). In fig. 7 we show the grid of iso-contours for the CC/NC-ratio and the Ge-production rate. The SNO (phase III) will measure the NC-event rate with 6% accuracy [47]. If we assume a reduced error of 5% for the CC-data then this makes the CC/NC error as 8% which can be compared to the present error of 11%. (This, in turn, reduces the absolute error in the CC/NC ratio down to 0.024 from the current value of 0.035.)

According to fig. 7, the current Ge production rate accuracy is $Q_{Ge} \approx 4 \text{ SNU}$. Using this accuracy and the expected SNO-III error, we find from fig. 7 the sensitivity (1% error) to \sin^2_{13} in the region $\sin^2_{13} \approx 0.03$:

$$(CC=NC + Ga) = 0.023: \tag{72}$$

It is only slightly better than the present one (66).

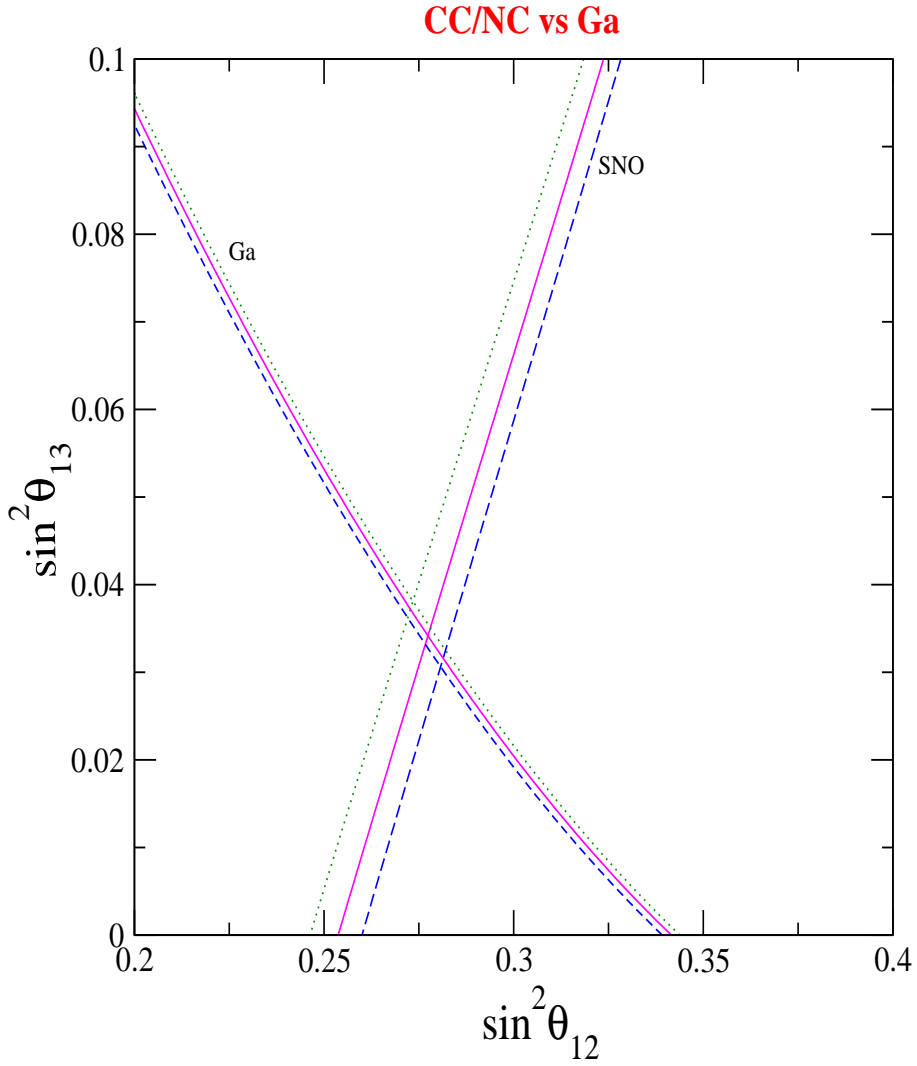


Figure 6: The iso-contours of $CC/NC = 0.31$ at SNO and $Q_{Ge} = 68.1$ SNU in Ga experiments in the $\sin^2 \theta_{12} - \sin^2 \theta_{13}$ plane for different values of m_{21}^2 : $m_{21}^2 = 9 \times 10^5 \text{ eV}^2$ - the dotted lines; $m_{21}^2 = 8 \times 10^5 \text{ eV}^2$ - the solid lines; $m_{21}^2 = 7 \times 10^5 \text{ eV}^2$ - the dashed lines.

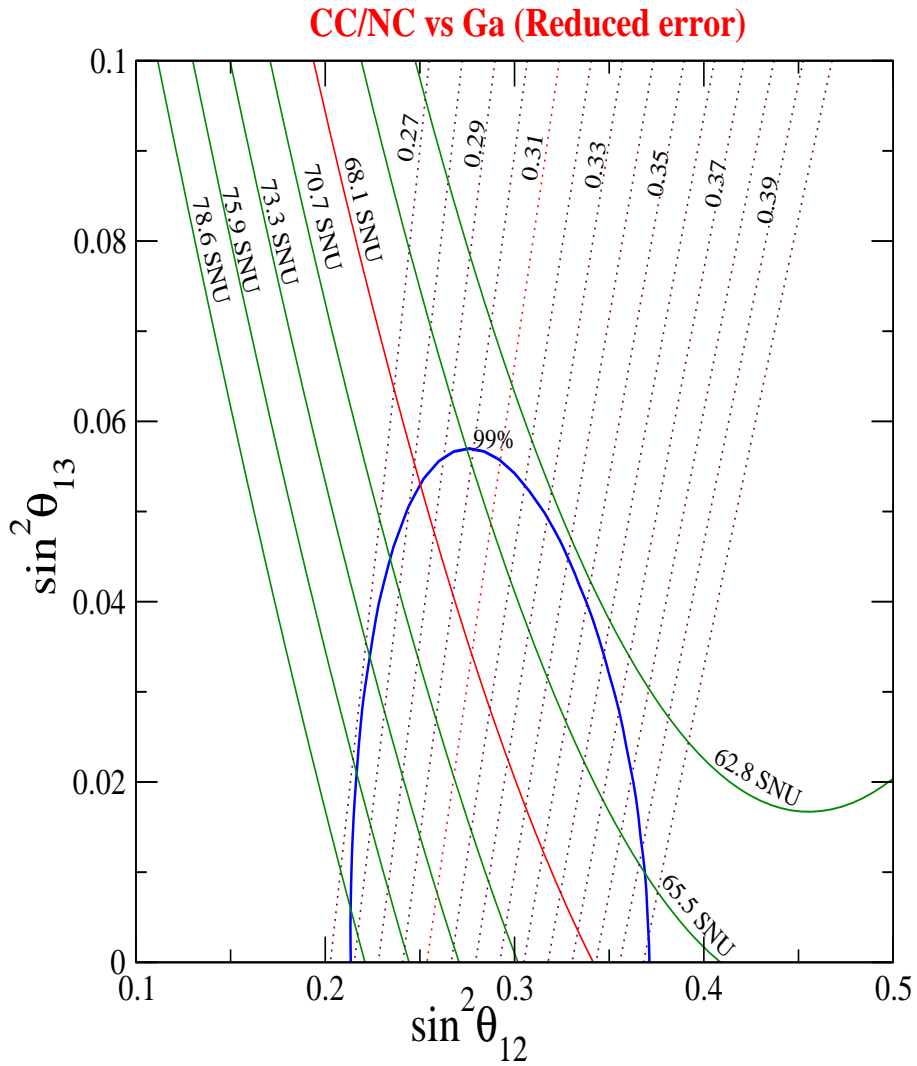


Figure 7: The iso-contours of the CC/NC ratio at SNO (dotted lines) and Ge-production rate Q_{Ge} (solid line) with reduced steps 0.01 and 2.6 SNU respectively, in the $\sin^2 \theta_{12}$ - $\sin^2 \theta_{13}$ plane. m_{21}^2 is held fixed at $8 \times 10^5 \text{ eV}^2$. The solid (blue) contour gives the 99% C.L. allowed area from the present global data.

If we use 5% accuracy for future possible measurements of CC/NC ratio and the Ge-production rate error 2.6 SNU (which could be the ultimate sensitivity of the Gallium experiments), then according to eq. 7, we obtain

$$(CC=NC + Ga) = 0.016: \tag{73}$$

In this case the value $\sin^2 \theta_{13} = 0.034$ would have 2:1 significance, and in the case of very small θ_{13} the upper bound will be $\sin^2 \theta_{13} < 0.024$ (0.048) at 90% (3 σ).

2). The Borexino and KamLAND plan to measure signal from the ^7Be neutrinos. The iso-contours can be well described by the low energy formula (57). Taking into account contribution from the non-electron (converted) neutrinos we find the iso-contours, R_{Borexino} , which coincide with iso-contours $hP_{eei} = C_{Be}$, where $C_{Be} = (R_{\text{Borexino}} - r)(1 - r)$.

The results of calculations are shown in eq. 8. The Borexino contours have similar form to those for Ga-rate.

Borexino is expected to accumulate 44000 events in 4 years of time (30 events/day) for LMA MSW solution. This corresponds to a statistical error of only 0.5% [48]. But the accuracy of measurement will be dominated by the background and systematics. Furthermore, the SSM prediction for the ^7Be flux has 10% uncertainty which will add to the total error unless one keeps the normalization of ^7Be flux as a free parameter to be determined from the Borexino experiment itself with a higher accuracy. Using eq. 8 we estimate that a 5% accuracy of measurements of the rate at Borexino will contribute to improvement of sensitivity of the solar studies to $\sin^2 \theta_{13}$.

3). New low energy solar neutrino experiments will be able to measure the pp-neutrinos with high accuracy [49]. Two kinds of experiments are being discussed [50] { one using the charged current reactions (LENS, MOON, SIREN) and the other using the electron scattering process (XMASS, CLEAN, HERON, MUNU, GENIUS).

For the pp-neutrinos we can use the iso-contour equation for the low energies as in (57) with substitution $C_Y = C_{pp} = hP_{eei_{pp}}$ and $\nu_{pp}^1 = hEV = m_{21}^2 i_{pp}$. Practically, ν_{pp}^1 is negligible.

In eq. 9 we show the contours of constant rate of the $e-e$ scattering events due to pp neutrinos. The neutral current contribution is also included. According to eq. 9, future measurements of CC/NC ratio with 5% accuracy and pp-rate with 2% accuracy will have a sensitivity (1 σ error)

$$(CC=NC + pp) = 0.015: \tag{74}$$

Consequently, the value $\sin^2 \theta_{13} = 0.034$ will be established with 2:3 significance, and in the case of very small θ_{13} the upper bounds $\sin^2 \theta_{13} < 0.022$ (0.045) at 90% (3 σ) can be achieved.

4). The future Megaton water Cherenkov detectors (HyperKamokande [51], UNO [52]) will be able to measure the ratio R_e with accuracy $R_e = 0.003$. We construct the fine grid of the R_e iso-contours for $f_B = 1$ (eq. 10). According to eq. 10 these measurements of R_e and pp-rate (2% accuracy) would have a sensitivity (1 σ error)

$$(CC=NC + pp) = 0.011: \tag{75}$$

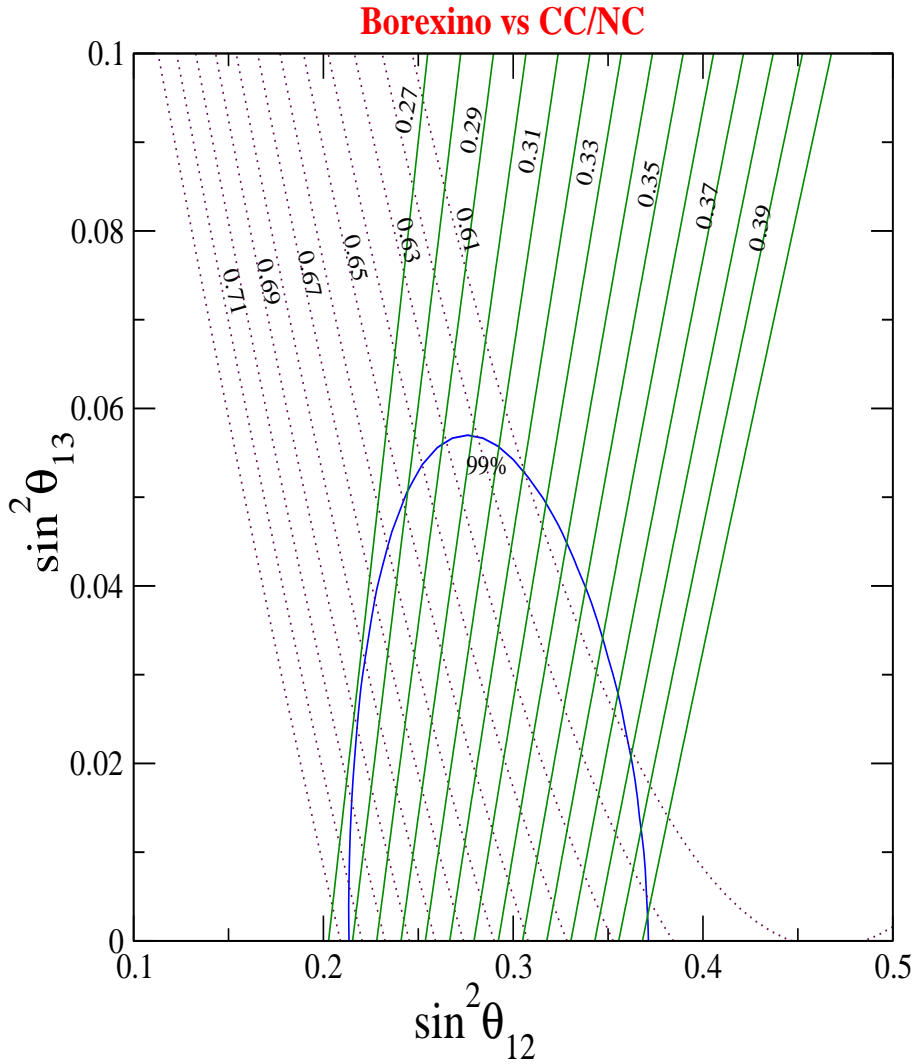


Figure 8: The iso-contours of Borexino rate suppression with respect to the SSM prediction in the $\sin^2 \theta_{12}$ - $\sin^2 \theta_{13}$ plane for $m_{21}^2 = 8 \cdot 10^5 \text{ eV}^2$. The solid (blue) contour gives the 99% C.L. allowed area from the global fit of all data.

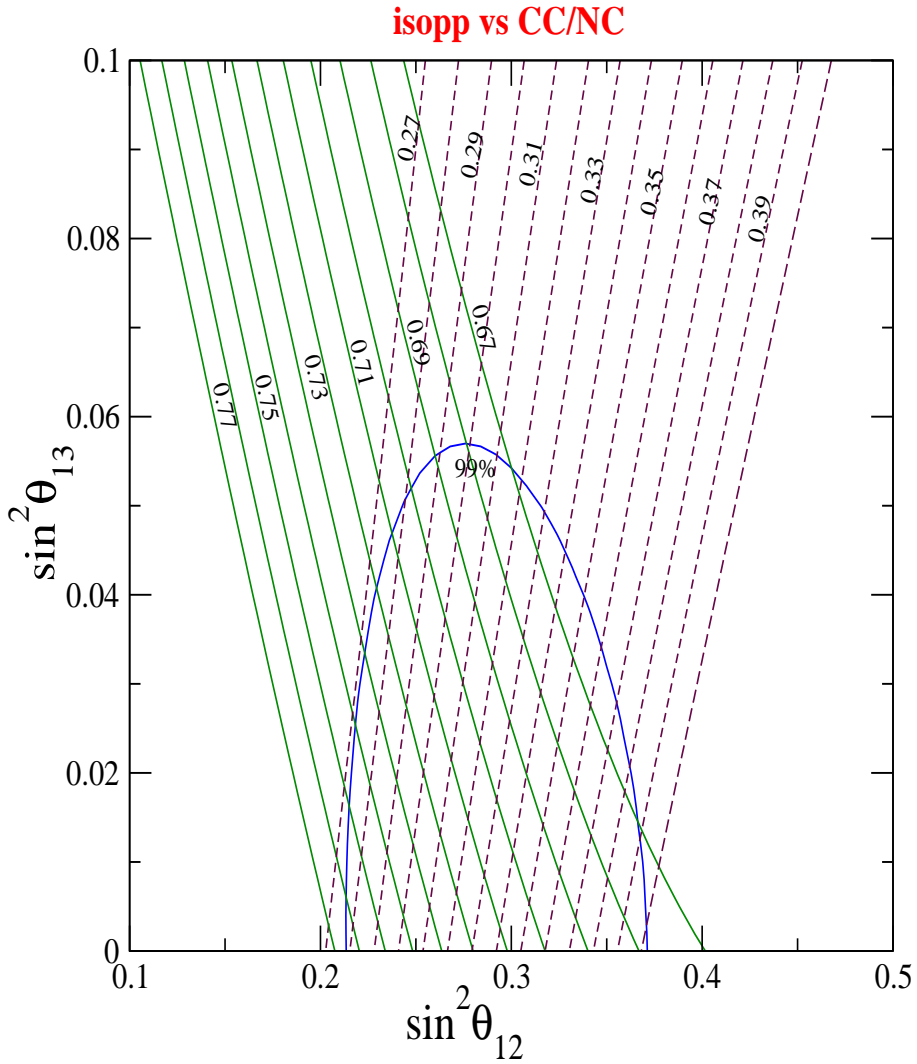


Figure 9: The iso-contours of the CC/NC ratio (dashed lines) and e scattering rate of pp neutrinos in the $\sin^2 \theta_{12}$ - $\sin^2 \theta_{13}$ plane for $m_{21}^2 = 8 \cdot 10^6 \text{ eV}^2$. The solid (blue) contour gives the 99% C.L. allowed area from the global fit of all data.

However, the problem here is the knowledge of f_B . It is difficult to expect that the accuracy of the theoretical predictions will be better than 10%. Comparable accuracy will be achieved in the direct measurements of the neutral currents. The global fit of the data including the spectral information and the regeneration effect with free f_B may give better accuracy.

So, we conclude that the future solar neutrino studies may reach a sensitivity $\sin^2 \theta_{13} = 0.015 - 0.020$, (1%), as compared with the present sensitivity 0.05 - 0.06. It seems that even combined fit of several future precision measurements will not go down to 0.01 which may be considered as an ultimate sensitivity of solar neutrino measurements of $\sin^2 \theta_{13}$.

On the basis of studies performed in sec. 5 and 6, we can identify signatures of the non-zero $\sin^2 \theta_{13}$. In general, they show up as a mismatch of the low and high energy measurements. Let us indicate several signatures.

1). Small value of the Ge production rate Q_{Ge} . For a given ratio CC/NC one can find the critical value of Q_{Ge}^c (CC=NC), so that inequality

$$Q_{Ge} < Q_{Ge}^c (CC=NC) \quad (76)$$

will testify for the non-zero value of $\sin^2 \theta_{13}$. From the fig. 7 we find $Q_{Ge}^c(0.30) = 76$ SNU, $Q_{Ge}^c(0.32) = 74$ SNU, $Q_{Ge}^c(0.34) = 72$ SNU, $Q_{Ge}^c(0.36) = 70$ SNU, etc.. The larger the difference in (76), the larger $\sin^2 \theta_{13}$. In fact, the present data satisfy the inequality (76), however the statistical significance is low. Apparently if CC/NC and Q_{Ge} are measured with high accuracy, the presence of non-zero $\sin^2 \theta_{13}$ can be established.

The inequality (76) can be inverted, so that small values of CC/NC for a given Q_{Ge} ,

$$CC=NC < CC=NC^c(Q_{Ge}); \quad (77)$$

testify for non-zero θ_{13} .

2). Similarly, small Borexino rate, R_{Bor} , will be an indication of $\theta_{13} \neq 0$:

$$R_{Bor} < R_{Bor}^c (CC=NC); \quad (78)$$

The critical Borexino rates for different values of CC/NC equal: $R_{Bor}^c(0.280) = 0.71$, $R_{Bor}^c(0.305) = 0.69$, $R_{Bor}^c(0.325) = 0.67$.

3). Small ν_e event rate produced by the pp-neutrinos, R_{pp} :

$$R_{pp} < R_{pp}^c (CC=NC) \quad (79)$$

is another signature. According to fig. 10 the critical values R_{pp}^c (CC=NC) equal 0.75 (0.294), 0.73 (0.318), 0.71 (0.343), 0.69 (0.373).

4). Weak spectrum distortion of the boron neutrinos. The spectrum distortion can be characterized, e.g., by the ratio of suppressions at low and high energies $r_R = R_e(E < 7 \text{ MeV})/R_e(E > 7 \text{ MeV})$. There is certain critical value of the distortion, r_R^c , which depends on CC/NC, so that weaker distortion will testify for non-zero 1-3 mixing. Indeed, for fixed CC/NC with increase of $\sin^2 \theta_{13}$, the 1-2 mixing, $\sin^2 \theta_{12}$, should increase (44) and therefore, the upturn of spectrum at low energies should be weaker.

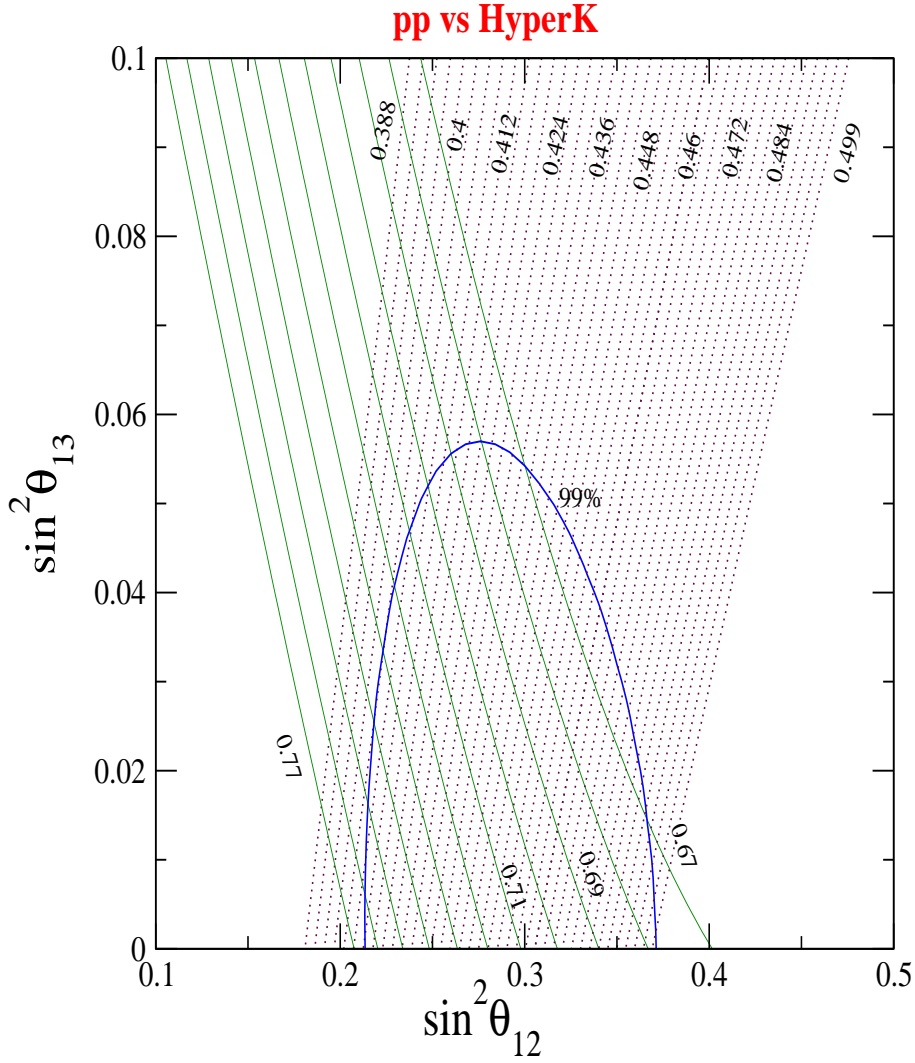


Figure 10: The iso-contours of the neutrino electron scattering rate for the pp neutrinos (solid line) and high energy ${}^8\text{B}$ neutrinos (dotted line) in the $\sin^2 \theta_{12}$ - $\sin^2 \theta_{13}$ plane. The iso-rates for the high energy neutrinos are drawn with a step 0.003 corresponding to the expected statistical error of a Megaton water detector like HyperK and Kamokande. m_{21}^2 is held fixed at $8 \cdot 10^5 \text{ eV}^2$. The solid (blue) contour gives the 99% C.L. allowed area from the present global fit of data.

7 Implications of the solar neutrino measurements of θ_{13}

Let us first compare sensitivities of future solar neutrino experiments with future sensitivity of reactor / accelerator experiments eqns. (4, 5, 6). With the expected errors for SNO-III 2% accuracy of the pp-neutrino flux measurements the solar neutrino experiments can reach sensitivity comparable to the one of the forthcoming MINOS and CNGS experiments. This sensitivity is at the level of the present bound from the global fit of all oscillation data and it is certainly worse than the sensitivity of future measurements.

The sensitivity would be comparable to that of J-PARC and Double-CHOOZ if the pp-neutrino flux is measured with 1% accuracy and CC/NC ratio – with 3% accuracy which looks rather unrealistic now.

Notice that survival probability P_{ee} does not depend on the CP phase δ , and therefore the problem of degeneracy with [53] does not arise. So, the solar neutrinos studies can provide a clean channel for determination of θ_{13} like the reactor neutrinos. Therefore, in spite of the lower sensitivity the solar neutrino data will contribute somehow to resolution of degeneracy of these parameters in the future global fits.

It seems that the reactor/accelerator experiments will obtain results much before future high statistics solar neutrino experiments will start to operate. In this case, possible implications of the solar neutrino measurements can include

- 1). Precise determination of $\sin^2 \theta_{12}$: resolution of the θ_{12} – θ_{13} degeneracy.
- 2). Comparison of results on θ_{13} (as well as on θ_{12}) from the solar neutrinos and reactor/accelerator experiments. The outcome could be further confirmation of the reactor/accelerator results by solar neutrinos, or establishing certain discrepancy which may imply new physics beyond the LMA solution of the solar neutrino problem.

Let us consider these two points in some details.

1). Resolving degeneracy of angles. Due to the strong $\sin^2 \theta_{12}$ – $\sin^2 \theta_{13}$ degeneracy unknown value of θ_{13} leads to the uncertainty in the determination of $\sin^2 \theta_{12}$ and vice-versa. Thus, in the CC/NC measurements, inclusion of the 1-3 mixing leads to increase of $\sin^2 \theta_{12}$ by 0.04 – 0.05 (that is, by 20%) if $\sin^2 \theta_{13}$ increases from 0 to 0.06 (see fig. 7). In the pp-neutrino flux measurements $\sin^2 \theta_{12}$ decreases by 0.06 – 0.08, when $\sin^2 \theta_{13}$ increases from 0 to 0.06 (see fig. 9). So, precise determination of $\sin^2 \theta_{12}$ ($\sin^2 \theta_{13}$) from the solar neutrino data is not possible unless $\sin^2 \theta_{13}$ ($\sin^2 \theta_{12}$) is measured or strongly restricted. As follows from our analysis a combination of high statistics measurement at high and low energies can remove the degeneracy.

2). Confronting the solar and reactor/accelerator results. If non-zero $\sin^2 \theta_{13}$ is measured our analysis will allow to understand relevance of the 1-3 mixing to the precision solar neutrino studies. For fixed m_{21}^2 , the 1-3 mixing will change determination of θ_{12} .

Notice that dependence of sensitivity of the solar neutrino studies to θ_{13} on the mass m_{31}^2 is very weak (via matter corrections to 1-3 mixing) in contrast to laboratory measurements. So, for small m_{13}^2 the former will have some advantage.

If θ_{13} effect is not found in future laboratory experiments and the upper bound at the level

$\sin^2_{13} < 0.01$ is established, the effect of 1-3 mixing will be irrelevant even for measurements with the 1% accuracy. The uncertainty of future measurements of 1-2 mixing \sin^2_{12} due to unknown \sin^2_{13} will be reduced down to 0.01. Furthermore, the precise measurements of \sin^2_{12} by CC/NC will have the smallest uncertainty due to larger slope of the iso-lines.

The analysis performed in this paper will allow us to understand new physics if inconsistencies in results of measurements will show up. Implications will depend on character of results, and in the positive case, on particular value of \sin^2_{13} . Comparing the laboratory bound with the results of solar neutrino studies one can realize new physics effects which may show up in the solar neutrinos only and can not be found otherwise.

Suppose, the precision solar neutrino measurements will give the nonzero value of \sin^2_{13} which is larger than the upper bound from the reactor/accelerator experiments. Such a situation may indicate some additional suppression of the solar neutrino flux at low energies. Indeed, this would shift the low iso-lines to the left - down. It would be equivalent of taking the low iso-lines in our plots (e.g., in fig. 3) with larger survival probability. The intersection with high energy iso-contours will shift down and therefore the inferred value of \sin^2_{13} will be reduced. This situation can be reproduced in the presence of sterile neutrino with $m^2 < 10^5 \text{ eV}^2$ [54]. In this case the extracted value of \sin^2_{12} reduces too.

Also agreement between the solar and laboratory measurements can be achieved by an additional suppression of the high energy (boron) flux due to flavor conversion, so that CC/NC lines move to the right - down. In this case also the intersection of the high and low iso-contours moves down and the inferred value of \sin^2_{12} increases. Such an effect can be produced by certain non-standard neutrino interactions.

The value of \sin^2_{13} extracted from the solar neutrino studies can be diminished if both the low and high energy fluxes are reduced by some additional mechanism. In fact, this imitates the effect of the 1-3 mixing and can be achieved by additional non-standard interactions.

Let us consider the opposite situation: \sin^2_{13} is discovered in the reactor/accelerator experiments, but the solar neutrino data prefer zero or smaller value of \sin^2_{13} . This can be explained if the survival probability is larger than the one predicted for given values of θ_{12} and θ_{13} . Again some scenarios with modified dynamics of conversion due to new interactions of neutrinos can reproduce such a situation.

Similarly discrepancy can be realized comparing values of the 1-2 mixing extracted from the solar neutrino data and reactor/accelerator experiments. Indeed, the \sin^2_{12} can be measured with 3% accuracy at 1 (1 d.o.f.) in the reactor experiments with baseline 50 - 60 km [55, 56, 38].

8 Conclusion

1). We have derived formula for the survival probability in the three neutrino context (34) which includes all corrections relevant for the future precision of measurements. We estimated the accuracy of approximation made.

2). In the three generation context in the first approximation (neglecting the matter effect on θ_{13}) the solar neutrino probabilities are functions of the mass split m_{21}^2 and the mixing angles: θ_{12} and θ_{13} . The split m_{21}^2 is already determined with a high precision by current data. Furthermore the survival probability has a weak dependence on this parameter in the allowed region. In view of this we have constructed plots in $\sin^2 \theta_{12} - \sin^2 \theta_{13}$ plane which clearly demonstrate the degeneracy of these mixing angles and also show how the uncertainty in one is going to affect the precision determination of the other. Synergy between the high and low energy solar neutrino flux measurement provides a better constraint on θ_{13} and allows us to resolve the degeneracy of these mixing angles.

3). Among the available solar neutrino data only the Ga experiment is sensitive to the low energy pp-neutrinos. Therefore we construct iso-rates of Ga experiments in the $\sin^2 \theta_{12} - \sin^2 \theta_{13}$ plane and investigate how the combination of these with the iso-rates of CL, SK and CC/NC ratio in SNO constrains θ_{13} .

At present the sensitivity of the solar neutrino experiments to θ_{13} is rather weak. A analysis of the solar neutrino data alone leads to non-zero best fit value: $\sin^2 \theta_{13} = 0.01$ which is not statistically significant. Larger value $\sin^2 \theta_{13} = 0.02$, follows from the fit of the solar data for $m^2 = 8 \cdot 10^5 \text{ eV}^2$ selected by the KamLAND experiment. The combination of the CC/NC at SNO and Q_{Ge} rate, which are less dependent on the solar neutrino fluxes, gives $\sin^2 \theta_{13} = 0.034 - 0.026$ (1).

At the same time, the global fit of all existing data (including reactor, accelerator and atmospheric neutrino results) leads to $\sin^2 \theta_{13} = 0.004$ as the best fit point and the upper bounds $\sin^2 \theta_{13} = 0.041$ (0.064) at 90% (3 σ) from the two parameter plots. Apparently CHOOZ and atmospheric data select smaller $\sin^2 \theta_{13}$ than it follows from the solar data. Being established in future high precision measurements such a mismatch may have very interesting implications.

4). The precision will improve with future accurate measurements of the pp-neutrino flux, the CC/NC ratio and the energy spectrum of events at high energies, etc.. We find that 5% measurement of the CC/NC ratio and 2% measurement of the pp-neutrino flux in the scattering will have a sensitivity $\sin^2 \theta_{13} \approx 0.015$ (1). The value $\sin^2 \theta_{13} \approx 0.01$ looks like the ultimate sensitivity which can be reached in the solar neutrino experiments of the next generation.

Since the probability involved is P_{ee} the problem of degeneracy with CP phase does not appear and solar neutrinos can provide a clean channel for θ_{13} measurements like the the reactor neutrinos.

5). It is likely that new accelerator/reactor results will be obtained first. Comparison of the results from solar neutrinos and accelerator/reactor experiments may confirm each other and further improve determination of $\sin^2 \theta_{13}$ or reveal some discrepancy which will indicate a new physics beyond usual interpretation of the solar neutrino anomaly.

Determination of $\sin^2 \theta_{13}$ will eliminate or reduce the $\theta_{12} - \theta_{13}$ degeneracy thus improving measurements of 1-2 mixing. Conversely, the better determination of $\sin^2 \theta_{12}$ can help in improving the precision of the $\sin^2 \theta_{13}$ measurements in the solar neutrino studies.

Comparison of the results of $\sin^2 \theta_{13}$ (as well as $\sin^2 \theta_{12}$) measurements in the solar neutrinos and in reactor and accelerator experiments may uncover new interesting physics beyond LMA

MSW picture which can not be found otherwise.

S.G. would like to thank The Abdus Salam International Centre for Theoretical Physics for hospitality and A. Bandyopadhyay and S. Choubey for using some of the codes developed with them. The authors are grateful to E. Lisi for valuable comments.

References

- [1] M. Apollonio et al., Phys. Lett. B 466 (1999) 415.
- [2] F. Boehm et al., Phys. Rev. D 62 (2000) 072002.
- [3] J. N. Bahcall, M. C. Gonzalez-Garcia, C. Pena-Garay, JHEP 0408, 016 (2004); [hep-ph/0406294].
- [4] A. Bandyopadhyay et al., hep-ph/0406328.
- [5] M. Maltoni, T. Schwetz, M. A. Tortola, J. W. F. Valle, New J. Phys. 6 122 (2004), arXiv:hep-ph/0405172 v3 (September 2004)
- [6] M. C. Gonzalez-Garcia, hep-ph/0410030.
- [7] S. Goswami, talk at Neutrino 2004, Paris, <http://neutrino2004.in2p3.fr>, hep-ph/0409224.
- [8] R. Saakian, Nucl. Phys. Proc. Suppl. 111, 169 (2002).
- [9] <http://projcngs.web.cern.ch/projcngs/>.
- [10] <http://jkjtokai.jaerigo.jp/>.
- [11] P. Huber, M. Lindner, T. Schwetz and W. Winter, Nucl. Phys. B 665 (2003) 487 [arXiv:hep-ph/0303232].
- [12] Letter of Intent for Double-CHOOZ F. Ardellier et. al., hep-ex/0405032.
- [13] H. Minakata, H. Sugiyama, O. Yasuda, K. Inoue and F. Suekane, Phys. Rev. D 68, 033017 (2003) [arXiv:hep-ph/0211111];
- [14] C. Lunardini and A. Y. Smirnov, JCAP 0306, 009 (2003) [arXiv:hep-ph/0302033].
- [15] M. Lindner, Int. J. Mod. Phys. A 18 3921, (2003) and references therein.
- [16] G. L. Fogli, E. Lisi, A. Marrone, D. Montanino, A. Palazzo, hep-ph/0104221.
- [17] G. L. Fogli, G. Lettera, E. Lisi, A. Marrone, A. Palazzo, A. Rotunno, Phys. Rev. D 66, 093008, (2002), G. L. Fogli, E. Lisi, A. Marrone, D. Montanino, A. Palazzo, A. M. Rotunno, Phys. Rev. D 69, 017301, (2004) [hep-ph/0308055].
- [18] J. N. Bahcall and C. Pena-Garay, JHEP 0311, 004 (2003) [arXiv:hep-ph/0305159].

- [19] M . C . Gonzalez-G arcia, C . Pena-G aray, Phys. Lett. B 527 199, (2002).
- [20] M . C . Gonzalez-G arcia, C . Pena-G aray, Phys. Rev. D 68 093003 (2003).
- [21] A . B . Balantekin, H . Yuksel, J. Phys. G 29 665, (2003).
- [22] M . M altoni, T . Schwetz, M . A . Tortola, J W F . Valle, Phys. Rev. D 68, 113010 (2003), M . C . Gonzalez-G arcia, M . M altoni, C . Pena-G aray, J W F . Valle, Phys. Rev. D 63 033005 (2001).
- [23] P . C . de Holanda, A . Yu. Sm imov, Astropart. Phys. 21, 287, (2004) [hep-ph/0309299].
- [24] P . C . de Holanda, A . Yu. Sm imov, JCAP 0302, 001, (2003); P . C . de Holanda, A . Yu. Sm imov, Phys. Rev. D 66, 113005, (2002).
- [25] A . Bandyopadhyay, S . Choubey, S . Goswami and K . Kar, Phys. Rev. D 65 (2002) 073031 [arXiv:hep-ph/0110307].
- [26] A . Bandyopadhyay, S . Choubey, R . Gandhi, S . Goswami and D . P . Roy, J. Phys. G 29, 2465 (2003) [arXiv:hep-ph/0211266]. A . Bandyopadhyay, S . Choubey, R . Gandhi, S . Goswami and D . P . Roy, Phys. Lett. B 559, 121 (2003) [arXiv:hep-ph/0212146].
- [27] A . Bandyopadhyay, S . Choubey, S . Goswami, S . T . Petcov, D . P . Roy, Phys. Lett. B 583, 134 (2004).
- [28] S . C . Lim , In Proc. of BNL Neutrino Workshop, Upton, NY , U SA 1987, edited by M . M urtagh, BNL-52079, C 87/02/05.
- [29] X . Shi, D . N . Schramm , Phys. Lett. B 283, 305 (1992), X . Shi, D . N . Schramm , J. N . Bahcall, Phys. Rev. Lett. 69, 717 (1992).
- [30] G . L . Fogli, E . Lisi, A . Palazzo, Phys. Rev. D 65, 073019 (2002), [hep-ph/0105080].
- [31] C . S . Lim , K . Ogure, H . T sujimoto, Phys. Rev. D 67, 033007 (2003), [hep-ph/0210066].
- [32] M . B lennow , T . Ohlsson and H . Snellman, Phys. Rev. D 69, 073006 (2004). [arXiv:hep-ph/0311098].
- [33] E . K h. Akhmedov, M . A . Tortola, J W F . Valle, JHEP 0405, 057 (2004), [hep-ph/0404083].
- [34] S . P . Mikheyev and A . Yu. Sm imov, Yad. Fiz. 42, 1441 (1985) [Sov. J. Nucl. Phys. 42, 913 (1985)]; Nuovo Cim . C 9, 17 (1986); S . P . Mikheyev and A . Yu. Sm imov, ZHETF, 91, (1986), [Sov. Phys. JETP, 64, 4 (1986)] (reprinted in "Solar neutrinos: the first thirty years", Eds. J. N . Bahcall et. al.).
- [35] A . Messiah, in Proceedings of the 6th Moriond Workshop On Massive Neutrino in Particle Physics and Astrophysics, ed. O . Fackler and J. Tran Thanh Van, 1986.
- [36] W . Haxton, Phys. Rev. Lett. 57 (1986) 1271; S . J . Parke, Phys. Rev. Lett. 57 (1986) 1275.

- [37] P. C. de Holanda, W. Liao and A. Y. Smirnov, Nucl. Phys. B 702, 307, (2004), [hep-ph/0404042].
- [38] A. Bandyopadhyay, S. Choubey, S. Goswami and S. T. Petcov, [arXiv hep-ph/0410283](http://arxiv.org/abs/hep-ph/0410283).
- [39] E. Keams, talk at Neutrino 2004, Paris, <http://neutrino2004.in2p3.fr>.
- [40] G. Gatta, talk at Neutrino 2004; T. Araki et al., hep-ex/0406035.
- [41] B. T. Cleveland et al., Detector, Astrophys. J. 496, 505 (1998).
- [42] J. N. Abdurashitov et al. [SAGE Collaboration], J. Exp. Theor. Phys. 95, 181 (2002) [Zh. Eksp. Teor. Fiz. 122, 211 (2002)] [[arXiv astro-ph/0204245](http://arxiv.org/abs/astro-ph/0204245)]. W. Hampel et al. [GALLIEX Collaboration], Phys. Lett. B 447, 127 (1999); C. Cattadori, Talk at Neutrino 2004, Paris, France,
- [43] S. Fukuda et al. [Super-Kamiokande Collaboration], Phys. Lett. B 539, 179 (2002) [[arXiv hep-ex/0205075](http://arxiv.org/abs/hep-ex/0205075)].
- [44] Q. R. Ahmad et al. [SNO Collaboration], Phys. Rev. Lett. 89, 011302 (2002) [[arXiv nuclex/0204009](http://arxiv.org/abs/nuclex/0204009)]. S. N. Ahmed et al. [SNO Collaboration], Phys. Rev. Lett. 92, 181301 (2004) [[arXiv nuclex/0309004](http://arxiv.org/abs/nuclex/0309004)].
- [45] J. N. Bahcall and M. H. Pinsonneault, Phys. Rev. Lett. 92, 121301 (2004) [[arXiv astro-ph/0402114](http://arxiv.org/abs/astro-ph/0402114)].
- [46] T. Araki et al., [KamLAND Collaboration], hep-ex/0406035 (v3).
- [47] K. Graham, talk at NOON 2004, February 11-15, 2004, Tokyo, Japan, <http://www-sk.icrr.u-tokyo.ac.jp/noon2004/>; H. Robertson for the SNO Collaboration, Talk given at TAUP 2003, Univ. of Washington, Seattle, Washington, September 5 - 9, 2003, <http://mocha.phys.washington.edu/taup2003>
- [48] C. Galbiati, talk at Neutrino 2004, Paris, <http://neutrino2004.in2p3.fr>.
- [49] M. Nakahata, Talk given at the Int. Workshop on Neutrino Oscillations and their Origin (NOON 2004), February 11 - 15, 2004, Tokyo, Japan.
S. Schonert, talk at Neutrino 2002, Munich, Germany,
- [50] see e.g., Y. Suzuki, talk given at Neutrino 2004, June 14 - 19 (2004) Paris, France.
- [51] T. Nakaya, presented at the XXth Int. Conf. on Neutrino Physics and Astrophysics, Munich, May 2002; Next-Generation Cherenkov Detector Hyper-Kamiokande, K. Nakamura, talk at Neutrinos and Implications for Physics Beyond the Standard Model 2002, <http://insti.physics.sunysb.edu/itp/conf/neutrino/talks/nakamura.pdf>.
- [52] UNO Proto-collaboration, UNO Whitepaper: Physics Potential and Feasibility of UNO, SBHEP-01-03 (2000), <http://nngroup.physics.sunysb.edu/uno/>; see also C. K. Jung 2002, hep-ex/0005046

- [53] V. Barger, D. Marfatia and K. Whisnant, *Phys. Rev. D* **65**, 073023 (2002) [[arXiv:hep-ph/0112119](#)].
- [54] P. C. de Holanda and A. Y. Smirnov, *Phys. Rev. D* **69**, 113002 (2004) [[arXiv:hep-ph/0307266](#)].
- [55] A. Bandyopadhyay, S. Choubey and S. Goswami, *Phys. Rev. D* **67**, 113011 (2003).
- [56] H. Minakata, H. Nunokawa, W. J. C. Teves and R. Zukanovich Funchal, [hep-ph/0407326](#).